universität wien

MASTERARBEIT / MASTER'S THESIS

Titel der Masterarbeit / Title of the Master's Thesis

"Feeding kinematics and skull morphology of the keeled box turtle *Cuora mouhotii* (Gray, 1862)"

verfasst von / submitted by

Valentin Blüml BSc

angestrebter akademischer Grad / in partial fulfilment of the requirements for the degree of

Master of Science (MSc)

Wien, 2019 / Vienna, 2019

Studienkennzahl lt. Studienblatt / degree programme code as it appears on the student record sheet:	A >066 831<
Studienrichtung lt. Studienblatt / degree programme as it appears on the student record sheet:	Masterstudium Zoologie
Betreut von / Supervisor:	Dr. Christian J. Beisser

Table of content

1. Abstract

The Genus *Cuora* (Geoemydidae) originates from an aquatic ancestor and includes aquatic, semiaquatic and terrestrial species. This ancestry indicates an inherited aquatic feeding mechanism. High speed cinematography was used to analyse terrestrial and aquatic feeding mechanisms of *Cuora mouhotii*. In addition, 3D reconstructions of the head based on microCT scans were prepared. This and previous studies show only slight morphological differences within *Cuora*. The data indicate that adaptations in hyoid morphology and the musculus adductor mandibulae complex seem to occur due to the diet and to a lesser extent due to the medium the species feeds in. The pterygoid, the basisphenoid and the supraoccipital show adaptations for broad insertions of the prominent adductor, which is responsible for jaw closing. This thick and voluminous muscle enables the crushing of hard prey such as snails. To examine feeding kinematics peaches and snails as soft and hard food sources were compared. Results show that the feeding cycle is composed of the ingestion, the manipulating phase and the transport phase. The latter is uniform for both food sources. The slow ingestion and manipulating phase displayed variability, thus indicating a prey-dependent modulation of the feeding behaviour, which is shown for the first time in *Cuora*. In contrast to all other investigated *Cuora* species, *C. mouhotii* was not able to feed under water, which indicates an evolutionary trend towards strictly terrestrial feeding.

1.1. Zusammenfassung

Die Nahrungsaufnahmemechanismen der Dreikiel-Scharnierschildkröte, *Cuora mouhotii* (Gray, 1862), als auch die Morphologie des Schädels wurden untersucht. Abstammend von einem aquatischen Vorfahren, teilen sich die rezenten Spezies des Genus *Cuora* in aquatische, semiaquatische und terrestrische Formen auf. Alle bisher untersuchten *Cuora* besitzen auch die Fähigkeit unter Wasser zu fressen. Um diese Fähigkeit als auch terrestrische Nahrungsaufnahmemechanismen zu untersuchen, wurde High-Speed-Kinematografie verwendet, zusammen mit microCT-Daten des Schädels von *C. mouhotii*. In der Morphologie des Schädels zeigten sich nur geringe Unterschiede zu anderen *Cuora* Arten. Anpassungen des Hyoidkomplexes als auch des Musculus adductor mandibulae scheinten auf die Nahrung zurückzuführen zu sein, und nur zum geringeren Teil auf das Medium, Wasser oder Luft. Gaumen, Basisphenoid und das Supraoccipital zeigten in *C. mouhotii* breite Ansatzstellen für einen kräftigen, voluminösen Adduktor, der für das Schließen des Kiefers zuständig ist. Um Schnecken zu knacken benötigen diese Schildkröten einen hohen Kraftaufwand, der durch den stark ausgeprägten Adduktor erzeugt wird. Für eine Analyse der Nahrungsaufnahmemechanismen wurden weiche Nahrung und harte Nahrung, in Form von Birnen und Schnecken, gegenübergestellt. Dabei wurde die gesamte Nahrungsaufnahme in Ingestion, Manipulationsphase und Transportphase, welche sich sehr uniform zeigte, eingeteilt. Die langsame Ingestion als auch die Manipulationsphase variierten in Geschwindigkeit und Länge und zeigten eine von der Beute abhängige Modulation des Freßverhaltens an, die zum ersten Mal in *Cuora* gezeigt wurde. Im Gegensatz zu allen anderen *Cuora* Arten, konnte *C. mouhotii* keine Nahrung unter Wasser aufnehmen. Deshalb könnte diese, den anderen *Cuora* Arten, in Bezug auf terrestrische Nahrungsaufnahme, einen evolutiven Schritt voraus sein.

2. Introduction

2.1. Turtle origins & formation of the Geoemydidae

Testudinata are a globally widespread group, which conquered aquatic and terrestrial habitats. Although many theories regarding their origin and sister group exist, molecular data support a split of the Archosaurians approximately in mid-Carboniferous (Shaffer et al., 2017). The earliest fossil records date back to the middle of perm (285-265 Mya) (Pereira et al., 2017). *Eunotosaurus africanus* (Seeley, 1892) in Zierman et al. (2019), marks the earliest turtle fossil, but is still called an intermediate stem turtle (*sensu* Joyce, 2015; Lyson et al., 2017). It fills an evolutionary gap between the separation of the Testudinata from the Archosauria and earlier fossils found (Pereira et al., 2017). For *E. africanus* a terrestrial setting is contemplated. The *Eunotosaurus* hypothesis is the most widely accepted regarding the origin of turtles. For a detailed review see Joyce (2015). *Odonthochelys semitestacea* (Carnium, 235-228 Mya) (Li et al., 2008) as well as *Pappochelys rosinae* (Ladinium, 242-235 Mya) (Schoch & Sues, 2015), two other stem lineage turtles, which appeared in the Triassic and still had an open shell, are in contrast thought to be semiaquatic, or at least foraged in areas with constant access to water (Schoch & Sues, 2015). It is likely that *Odontochelys* could have been a terrestrial species (Joyce, 2015), and although Li et al. (2008) suggest a marine or an aquatic habitat, morphological adaptions as well as terrestrial fauna in sediments indicate a clear preference for a terrestrial habitat. The earliest completely shelled turtles, which occurred in the late Triassic, were shown to be terrestrial (*Palaeochersis talampayensis,* 235-201 Mya) (Joyce & Gauthier, 2004). This turtle ancestor seems like the last terrestrial group up to the formation of the Testudinidae, which are within the crown turtles. Nevertheless, the last common ancestor of all crown turtles, Pleurodira as well as Cryptodira, is described as living in fresh water (Joyce & Gauthier, 2004). The split into Cryptodirans and Pleurodirans from the turtle stem lineage occurred in the late Triassic to the early Jurassic (Crawford et al., 2015; Joyce et al., 2016; Pereira et al., 2017). Splitting the Durocryptodirans in two lineages about 110 Mya in the middle Cretaceous resulted in the appearance of Americhelidia on the one hand and of Testudinoidea on the other. Within the Cryptodirans, terrestrial species only occur in the Testudinoidea. They consist of two major groups, the Emysternia (Emydidae, Platysternidae) and the Testuguria (Testudinidae, Geoemydidae) (Crawford et al., 2015; Pereira et al., 2017). The small group of the Platysternidae, consisting of just one species (Rhodin et al., 2017), is purely aquatic, whereas in all other Testudinoidea families purely terrestrial species occur as well. Testudinidae are solely terrestrial, but Emydidae and Geoemydidae consist of aquatic, semiaquatic as well

as terrestrial species (Fritz & Havaš, 2007). Molecular data combined with biogeographical data show that the last common ancestor of Emysternia and Testuguria appeared 92 Mya ago. The Testuguria, which split up about 74 Mya in the late Cretaceous, include the Geoemydidae (Pereira et al., 2017), and, as a member of this family, the investigated species *Cuora mouhotii*. Molecular data support the placement of the earliest fossils of Geoemydids found in Asia in the Eocene (Claude & Tong, 2004; Shaffer et al., 2017). Several authors illustrated the monophyly of this family using molecular data (Sasaki et al., 2006; Le & McCord, 2008).

2.2. Feeding mechanisms in turtles

Tetrapods display distinct feeding mechanisms, which are generally structured in phases, namely ingestion, intraoral transport, manipulation (mechanical reduction/processing) and swallowing. These phases are not strictly separated but rather show a fluent transition. A hypothetical general feeding cycle can be applied to all tetrapods, which is then modified depending on different parameters like habitat and medium (Bramble & Wake 1985; Hiiemae & Crompton, 1985; Schwenk, 2000). The feeding cycle in turtles reflects the same scheme, resulting in medium specific feeding mechanisms (Wochesländer et al., 1999; Wochesländer, et al., 2000; Wyneken et al., 2008; Natchev et al., 2015).

Some studies underline, that the transition from water to a terrestrial habitat and with that terrestrial feeding strategies occurred at least four times within different turtle lineages (McCord et al., 2000; Feldman & Parham, 2002). This refers to the Testudinidae, *Rhinoclemmys*, *Terrapene*, and *Cuora*. Terrestrial food uptake stands in complete contrast to aquatic feeding mechanisms because the medium's density and other physical parameters differ markedly. This leads to the necessity of variable movements of the jaw, hyoid and tongue for a successful feeding procedure in the respective medium (Schwenk, 2000; Bels et al., 2008).

Testudinidae show different approaches of terrestrial ingestion, which is defined by the intake of food into the oral cavity (for review see Lemell et al., 2019). Distinct forms of terrestrial ingestion are distinguishable within the group of Testudinoidea. First, jaw prehension, a method in which the jaw itself grasps the food, as seen in Geoemydidae. This is followed by lingual transport of the food items into the mouth. Emydidae show a slight difference of the described mode, a slight protraction of the tongue appears during jaw prehension (Natchev et al., 2015; Kummer et al., 2017). In contrast, Testudinidae use their tongue for food uptake, called lingual prehension. The rough surface of the tongue builds up adhesive forces between the tongue and the food item, which is then grasped by the tongue and in combination with the jaws pulled inside the oral cavity (Wochesländer et al., 1999; Natchev et al., 2010). A different mechanism

is carried out by Emydids and Geoemydids namely ingestion by the jaws without using the tongue.

In an aquatic environment, a different ingestion mechanism, namely suction feeding, is used (for review see Schwenk, 2000; Lemell et al, 2019). A quick increase of volume in the oral cavity, and thus a negative pressure, results in an inflow of water into the oral cavity, creating suction forces, via a quick depression of the hyoid complex. Bearing in mind that the prey has about the same density as water, this inflow entrains the prey. Slow outflow of water through the mouth follows the ingestion. The lack of gills, unlike in fish, leads to a bidirectional water flow during suction feeding, where the water has to leave the mouth the same way it entered (Lemell et al., 2002; Lemell et al. 2019). Suction feeding can either be conducted in the form of compensatory suction feeding, where suction forces compensate the bow wave generated by the head extension, or by sucking the food into the oral cavity. Often, both modes are combined (Bels et al., 2008). Generally, the ingestion is then followed by cyclic phases of manipulation of the food and further transport to the oesophagus (Natchev et al., 2009). These phases following the ingestion can vary and are not uniform across different taxa (Schwenk, 2000; Bramble & Wake, 1985).

2.3. Morphological adaptations to the medium

To vary behaviours and mechanics of the feeding process, morphological variations, especially of the head and neck, are necessary. Terrestrial as well as aquatic environments require certain adaptations in skull shape and feeding strategies (Claude et al., 2004). However, only slight changes in skull morphology are required when switching dietary preferences, from a specialised diet to a more generalised or vice versa (Foth et al., 2017). Nevertheless, it is hard to directly conclude a habitat and diet preference only by investigating the skull morphometries and shape of an extinct or extant turtle species (Claude et al., 2004).

General morphological aspects of tetrapod aquatic and terrestrial feeders have been studied intensively (Bramble & Wake, 1985; Heiss et al., 2018; Natchev et al., 2015; Schwenk & Rubega, 2005). For instance, thickness as well as the curvature of the palatine differ depending on the medium. For the genus *Cuora* it has been shown that aquatic species like *C. amboinensis* possess a flattened palate (Natchev et al., 2009). A flat palate would reduce turbulences in the oral cavity, thus enhancing the directional flow of water and the prey into the oral cavity (Lemell et al. 2000). In contrast to that, *C. flavomarginata*, which is thought to be a more terrestrial species, has a more concave form of the palate. *C. galbinifrons*, another highly terrestrial species of this group, also displays a dorsally concave palate (Natchev et al., 2009). For *Cuora*

this does indicate a palate shape dependent on the preferred medium for feeding. Differences in palate tickness do occur regarding the hardness of the diet (Claude et al., 2004), but this parameter was not measured for *Cuora*.

So far, the hyoid complex has been studied intensively in turtles. Aquatic forms and foremost marine turtles often possess a thick and robust hyoid apparatus. Enlarged and ossified branchial horns broaden the ventral neck posterolateral, and thus are able to increase the overall volume of the oral cavity during suction feeding (Lemell et al., 2002; Bels et al., 2008). Geomydids slightly differ from this concept, especially *Cuora.* Within this genus, the hyoid seems rather robust, only small differences between aquatic and terrestrial species occur. Ossification of the hyoid complex in Geoemydids seems to be determined by taxon and age and to a lesser extent by the medium (Richter et al., 2007). For *C. galbinifrons,* it has been shown that its flattened cornu branchiale II, which stretches far posterior, is additionally attached laterally to the oesophagus (Natchev et al., 2010).

Certain *Cuora* species have already been studied. The first one has been *C. amboinensis* (Wochesländer et al., 2001, Natchev et al., 2007), which has been shown to feed both on land and in water. Natchev et al. (2007) did follow up this pioneering study in *Cuora* feeding mechanisms and continued his studies on *C. galbinifrons* and *C. flavomarginata*. All three species can feed in both media, water and air. *C. amboinensis* prefers aquatic habitats, whereas *C. flavomarginata* rather feeds terrestrial. *C. galbinifrons* is the most terrestrial *Cuora* species of the three researched (Natchev et al. 2007, 2009, 2010). Further studies on these species have been carried out regarding the tongue morphology and its connection to feeding strategies, environments and mechanism (Beisser et al., unpublished data). Generally, the genus *Cuora* proves to be a good example for investigating certain aspects of the aquatic-terrestrial transition in amniotes. Within one genus every form of habitat preference is present.

2.4. *Cuora mouhotii*

Cuora mouhotii mouhotii (Gray 1862), formerly known as *Pyxidea mouhotii* and at first description *Cyclemis mouhotii* in (Gray, 1870), is a species within the Geoemydidae (Fritz & Lehr, 1998; Fritz & Havaš, 2006; Rhodin et al., 2017). Its common name "Keeled Box Turtle" indicates that its keels on the back, one in the middle as well as two smaller ones laterally on the carapax, are eponymous. Recent findings have shown that this species is highly terrestrial and not, as some suspected, semiaquatic (Fischer et al., 2010). Here, I am defining “semiquatic” as behavioural patterns of a species which are carried out in water, whether it is feeding or other behavioural traits. Individuals have never been observed in water (Xiao et al., 2017a), but they

sometimes appear in the nearer distance around streams and lakes (Platt et al., 2013) and therefore were thought to be semiaquatic. Geographic documentation of the species range is unfortunately quite insufficient, because individuals are hard to find in the wild. Nevertheless, assured distribution ranges from Bhutan to central Vietnam, and covers parts of many countries including Bangladesh, China, India, Laos, and Myanmar (Fritz et al., 2002; Struijk et al., 2016b; Das et al., 2016; Rhodin et al, 2017). Different hybridization events of *C. mouhotii* have been reported by Stuart & Parham (2004), Shi et al. (2005) and Struijk & Blanck (2016a) with *C. galbinifrons*, *C. bourreti*, *C. trifasciata* and *C. picturata*.

Despite its dorsal keels, *C. mouhotii* has other different phenotypic features, like its serrated hind marginals, its posterior widening carapace and its narrow and long nuchal scute (Das et al., 2016). Midline carapace length can vary but is approximately 185 mm in wild adult individuals. Carapace colour ranges from light brown (Fig. 1) to nearly black. Between the hyo- and hypoplastron, a hinge with kinetic function exists, but still the species cannot retract its whole body into the shell (Das et al., 2016). Prominent head features are the hooked lower jaw and the large jaw adductor musculature.

Fig. 1 Habitus of *Cuora mouhotii*, visualized by a specimen from the Zoo Schönbrunn, Vienna. A prominent feature are the serrated hind marginals and the dorsal keel spanning from anterior to posterior medially over the carapace.

In general, the habitat of the species is not exclusively limited to one particular environment. Tropical moist forests are the most common habitat, whereas members of the species in Vietnam show a preference for broadleaf evergreen forests. Especially in some very dry Vietnamese areas, they were observed near river valleys, where water is present (Platt et al. 2013, Wangyal et al. 2012). It has never been observed that *C. mouhotii* entered water in the wild, although in captivity, they sometimes bath or soak themselves when stressed and/or the temperature is too high (Struijk et al., 2016b). Activity patterns in this species differ over the span of a year. Their height are reached during the rainy season, in the warmer period of the year. During other periods, the activity decreases drastically and they often burrow themselves

and persevere (Wang et al., 2011; Das et al., 2016). Many different threats have led the species to the rim of extinction. Thus, *C. mouhotii* is listed as endangered in the IUCN red list of threatened species (Asian Turtle Trade Working Group, 2000). Habitat loss as well as poaching for traditional Chinese medicine, pet trade, turtle farms and food create an immense pressure on almost every chelonian species (Shi et al., 2008). These threats are referred to as the "Asian turtle crisis", over all resulting in smaller populations in different asian chelonian taxa. Due to its big range and the difficulties in finding *C. mouhotii* in the wild, the actual population cannot be estimated, but market trades have shown that between 1998 and 2001 about 170.000 - 290.000 specimen were traded (Zhou & Jiang, 2008).

2.5. Aims of this study

This study aims to give light to the food intake mechanisms of *Cuora mouhotii* by using high speed kinematics. Subsequently, these findings are supplemented with a microCT scan of the skull, to demonstrate its head morphology. This sheds light on the question whether the head morphology resembles one of a terrestrial turtle or one of a semiaquatic or even aquatic species. *C. mouhotii* is considered a highly terrestrial species and therefore should not be able to feed under water, whereas Natchev et al. (2009) has shown that the terrestrial *C. galbinifrons* still possesses under water feeding mechanisms. All crown turtles are reported to be of aquatic ancestry. It will therefore be explored if it is plausible that *Cuora* species still possess an inherited aquatic feeding mode.

In addition, *C. mouhotii* is known to feed on a wide ranging, mostly carnivorous diet, including snails as well as softer prey. To identify if there are any differences between soft and hard food, two prey types were presented during filming. This study aims to expand the already existing knowledge about *Cuora* feeding mechanisms and to contribute to new insights into the evolution of terrestrial feeding in this genus.

3. Material and Methods

Three individuals of *Cuora mouhotii* were used in this study. They were borrowed from the Zoo Schönbrunn in Vienna. All of them were adult females. Stacks of two individuals were kept for about four weeks at the University of Vienna. To prevent any further stress for the turtles, the whole terrarium, where they were kept at the Zoo, was transported to the university. The terrarium measured 1 meter in length, 70 cm width and 30 cm in height. The filling consisted of a thick layer of soil, dried plants and some chunks of bark. Water, which was regularly changed, was presented in a bowl with a diameter of about 15 cm and a height of 2-3 cm. In contrast to the feeding for the filming, feeding routines at university every 2-3 days consisted of bananas, peaches, cucumbers, tomatoes, snails, slugs, *Zoophoba sp*. larvae and mealworms. Day and night rhythm was about 12 hours dark to 12 hours light. The room had a temperature of 23-25°C. The three individuals investigated measured between 15 and 17 cm in carapace length.

3.1. High speed cinematography

Each individual was filmed in a glass terrarium which was 55 cm length, 30 cm wide and 30 cm in height. The videography itself was carried out via a Photron Fastcam 1024PCI (Model: 100K; Photron Ltd; Tokyo, Japan) equipped with a Nikkor 24-85 mm 1:2, 8-4 D lens (Nikon, Tokyo, Japan). The whole system was kept steady on a Manfrotto tripod. The length of the terrarium was in parallel with the longer side of the sensor of the camera, to film the turtles laterally. Food as well as the animal had to be clearly visible during the whole feeding process, so the camera was positioned at the eye level of the turtle. To prevent any disturbances, the sides of the terrarium were hanged with clothes. Recording was carried out via the program Photron Fastcam Viewer (Version 3.6.0). To shorten the frame amount and the framerate, in some 500 fps (frames per second) films the open source program Virtualdub (Version 1.10.4) was used. In those films every second frame was cut out, to get a frame rate of 250. Generally, the films were shot at 250 frames per second, with a shutter speed of 1/1000 of a second at f8 (lens). To brighten up the terrarium, one Dedocool COOLt3 light spot (Dedolight Dedocool, Dedo Weigert Film GmbH, Germany) was used. The scene was lit from the same general direction as the camera, only slightly higher and a bit to the side. To enhance visibility of the feeding process, a white paper was put underneath the terrarium to act as a reflector and shine light at the ventral parts of the turtle.

Terrestrial feeding in *Cuora mouhotii* was investigated with two different food sources. On the one hand soft food, in form of peaches, and on the other hand hard food, consisting of snails. The pieces of peach and snails were approximately 1 cm^3 in size. Both were presented at the same location for all three individuals.

Aquatic feeding was conducted at different water levels at varying temperatures. First, water temperatures of about 23-25 °C were tested, afterwards the temperature was raised to 27-29 °C. The terrarium was filled with 4-8 cm of water, so the turtle could still reach to the ground with its feet. To accustom the tortoises to water, they were slowly trained to get comfortable in that medium, at start without food, and then after some training sessions with food. Aquatic feeding was conducted with different food sources. The question was not if they behave differently but if they are able to feed under water at all. Like in the terrestrial setup the food was presented on the same location. Floating food items were presented and pressed under water with a forceps, which was key to investigate the food uptake mechanism under water.

3.2. Analyses

The analytical part was done with a MATLAB (The Mathworks Inc., Natick, MA, USA) based program provided by Christian Beisser, which tracks different points on each frame of the film. The points set were on the upper jaw, lower jaw, tympanon, carapax, tongue and on the food (Fig. 2). The hyoid was not tracked due to difficulties with head movements during the feeding process. Visibility of the hyoid was not given most of the time, because of neck retraction. Tracking points were then analysed to create average value graphs, as well as speed and time measurements. Based on these tracking points, several kinetic variables could be analysed for the three different phases, namely ingestion phase, manipulation phases (MP), and transport phases (TP). These variables consisted of the angle of the maximum gape (MG), head movement and tongue movement. Additionally, duration as well as mean velocity and the maximum velocity of the ten highest velocities averaged, were measured for these movements. Mean value graphs were done for all investigated cyclic behaviours, including ingestion, MP and TP.

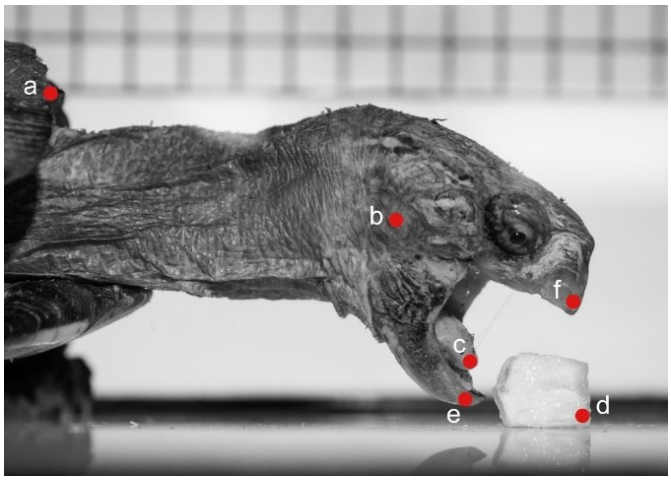

Fig. 2. *Cuora mouhotii* feeding on a piece of peach, displayed during the mouth opening of the ingestion. Marked in red are the points tracked. (a) carapace, (b) middle of the tympanon, (c) tip of the tongue, (d) food, (e) tip of the lower and (f) upper jaw.

3.3. MicroCT & skull reconstruction

For the microCT scan, an individual of the Natural History Museum Vienna was used (Natural history museum inventory number: NMW 40485: 1). The skull was cut off and fixated with 70% alcohol for one week and in 4% Formaldehyde for 5 weeks. The MicroCT Scans were carried out on a Scanco µCT 35 in the fashion of a dual energy Scan, where two different X-ray energy spectra are used, 40 kVp and 80 kVp (Handschuh et al., 2017). Basis material decomposition resulted in three material fractions, representing different materials or tissues. The background fraction (signal for ethanol) was used to reconstruct soft tissues like muscles, ligaments/tendons, nerve tissues and glands. The fraction of hydroxiapatit showed bony elements, whereas the iodine fraction represented stained soft tissues. The reconstruction was done with the program Amira 6.3 and 6.4 (Mercury Systems). Further 3D visualisations in form of volume renderings were carried out via Amira and Drishti 2.4 and 2.6 (Limaye, 2017). Figures of 3D visualisations displaying a white background were carried out via Drishti, the ones with a black background were done in Amira. The fraction for iodine was used for comparison, to get clarification on different tissues and structures in the background scan.

For uniformity, nomenclature of muscles and tissues follows the structure as proposed by Werneburg (2011), who used a numbering system for all muscles, following an order regarding their innervation of the cranial nerves I-XII. To get a better understanding of different muscle complexes, the brain and its nerves were reconstructed as far as the resolution made it possible. Hence, the cranial nerves, especially nervus trigeminus, which reaches to the adductor mandibulae musculature, helped resolve the different portions of this muscle complex (Holliday & Witmer, 2007; Werneburg, 2011). To increase the informative value of the reconstruction, the main eye muscles were reconstructed as well.

4. Results

4.1. Morphological analyses

In addition to the 3D visualisation, a dissection of the skull's musculature was conducted.
A complete list of the abbreviations is listed at the end of the thesis (P. 67 and 68).

4.1.1. Skull

As expected, the skull of *C. mouhotii* is anapsid and akinetic. The skull is approximately twice as long as wide (Figs. 3; 4), whereas its height is slightly smaller than its width. Lengthwise it measured 35 mm from the most anterior part of the upper jaw to the joint of the basioccipital with the first vertebrae. In general, its appearance is very robust. The dorsal and the ventral view show a pointed form of the snout region, whereas viewed laterally it is rounded (Figs. 3; 4). Prominent bones are the supraoccipital with a slight dorsal spike, as well as the parietals, which are, compared to other *Cuora* spp. elongated posteriorly and dorsally (Fig. 3). Another striking feature is the long anterior part of the pterygoid, the processus pterygoideus, which reaches ventrally and builds a part of the eye capsule and the oral cavity, an important muscle attachment site (Fig. 3). In the mediodorsal oral cavity the basisphenoid shows a keeled form which reaches anterior (Fig. 4. b).

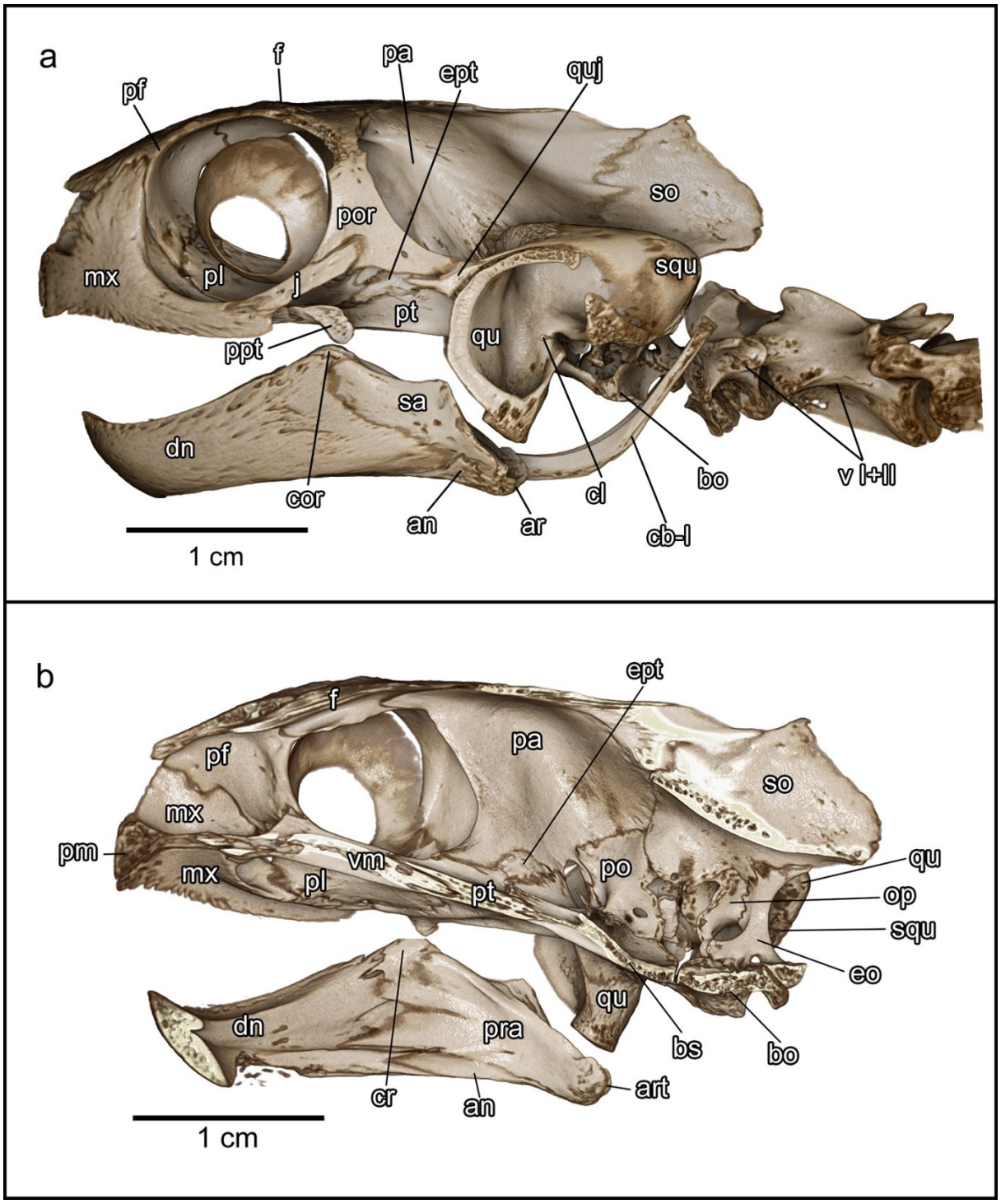

Fig. 3. 3D visualisation of the skull of *C. mouhotii*. Only ossified elements of the skull are shown. (a) lateral view; Note the anterior processus of the pterygoid. (b) A virtual sagittal cut was carried out. The vertebrae as well as the cornu branchiale-I were removed for clarity reasons. **an**, angular; **ar**, articular; **bo**, basioccipital; **bs**, basisphenoid; **cb-I**, cornu branchiale-I; **cl**, columella; **cr**, coronoid; dn, dental; **eo**, exoccipital; **ept**, epipterygoid; **f**, frontal; **j**, jugal; **mx**, maxilla; **op**, opisthotic; **pa**, parietal; pf, praefrontal; **pl**, palatine; **pm**, premaxilla; **po**, prootic; **por**, postorbital; **ppt**, processus pterygoideus; **pra**, prearticular; **pt**, pterygoid; **qu**, quadratum; **quj**, quadratojugal; **sa**, surangular; **so**, supraoccipital; **squ**, squamosal; **vI+II**, vertebrae I + II; **vm**, vomer.

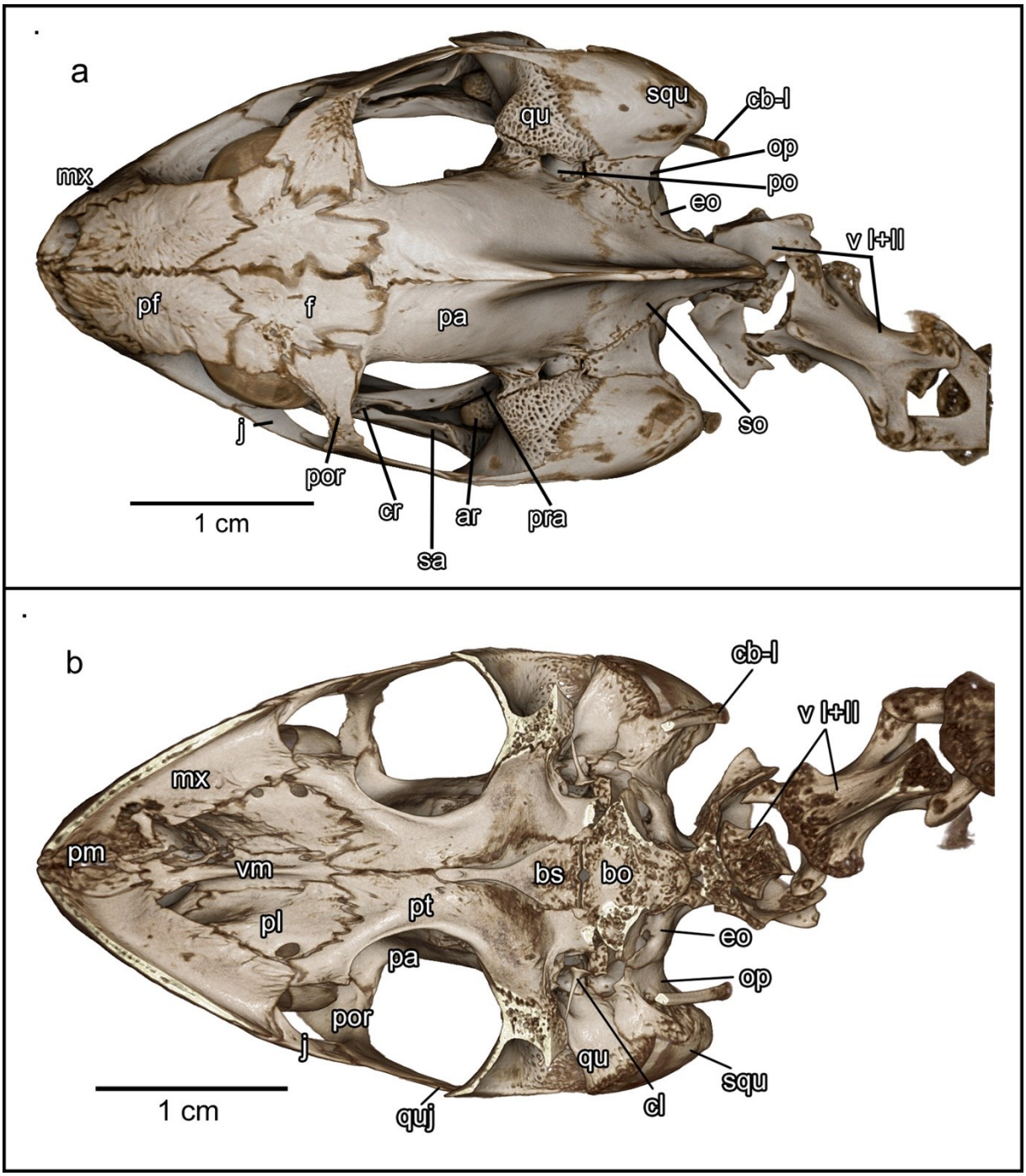

Fig. 4. 3D visualisation of the skull of *C. mouhotii*. (a) Dorsal view of the skull (b) Ventral view, with an anterioposterior section through the quadratum to remove the lower jaw, cb-I and parts of the quadratum, to increase visibility on numerous other structures. **ar**, articular; **bo**, basioccipital; **bs**, basisphenoid; **cb-I**, cornu-branchiale-I; **cl**, columella; **cr**, coronoid; **eo**, exoccipital; **f**, frontal; **j**, jugal; **mx**, maxilla; **op**, opisthotic; **pa**, parietal; **pf**, prefrontal; **pl**, palatine; **pm**, premaxilla; **po**, prootic; **por**, postorbital; **pra**, prearticular; **pt**, pterygoid; **qu**, quadratum; **quj**, quadratojugal; **so**, supraoccipital; **squ**, squamosal; **sa**, surangular; **v I+II**, vertebrae I+II; **vm**, vomer.

Elements of the Hyoid apparatus

The hyoid complex itself shows bony and cartilaginous elements and fills a big portion of the mouth floor (Figs. 5). It does not seem very robust in this specimen with only one ossified element, the cornu branchiale-I (cb-I). Most of its parts are built of cartilage and thus it has a flexible appearance.

Corpus hyoidei

The unpaired cartilaginous corpus hyoidei covers most of the oral cavity ventrally. Anterio-laterally attached are the cornua hyalia which reach dorsally (Fig. 5). Medially the corpus hyoidei is connected to the paired cb-I. The corpus hyoidei is posteriorly connected to the cornu branchiale-II (cb-II). The hypoglossum lies dorsally of the anterior part of the corpus hyoidei. The processus lingualis reaches medially further rostral. The trachea lies in the convex fold in the centre of the corpus hyoidei (Fig. 5. b).

Cornu branchiale-I

The only ossified hyoid structures are the paired cb-I (Figs. 3; 5). Between the lower jaw, both cb-I lie laterally, mediad to the prearticular and angular, and extend further posterior and turn dorsally till they end posterior to the squamosal (Fig. 3) On the anterior end a small cartilage connects them to the corpus hyoidei. The cb-I, round in cross-section, connect posterior with the cartilaginous epibranchiale-I (Fig. 5), which extends further caudal and reaches dorsally above the first vertebrae.

Cornu branchiale-II

The cb-II, cartilaginous structures, are posterior to the corpus hyoidei. At first the cb-II follow the path of the cb-I posteriorly but remains medioventrally. In cross-section they are horizontally flattened (Fig. 5).

Hypoglossum

The lateral broad, cartilaginous hypoglossum is situated ventral of the corpus hyoidei and partly closes the oral cavity ventrally. Its processus reaches into the tongue rostrally, a bit further anterior than the processus lingualis (Figs. 5.a; 15).

Cartilago thyreoidea

In the groove of the corpus hyoidei the cartilago thyreoidea (Fig. 5.a, b; 15) builds up the part where air enters (rima glottis) the proximal situated trachea. Laterally, the walls of the glottis are built by two small cartilages. Anteriorly it is closed in a rotund shape.

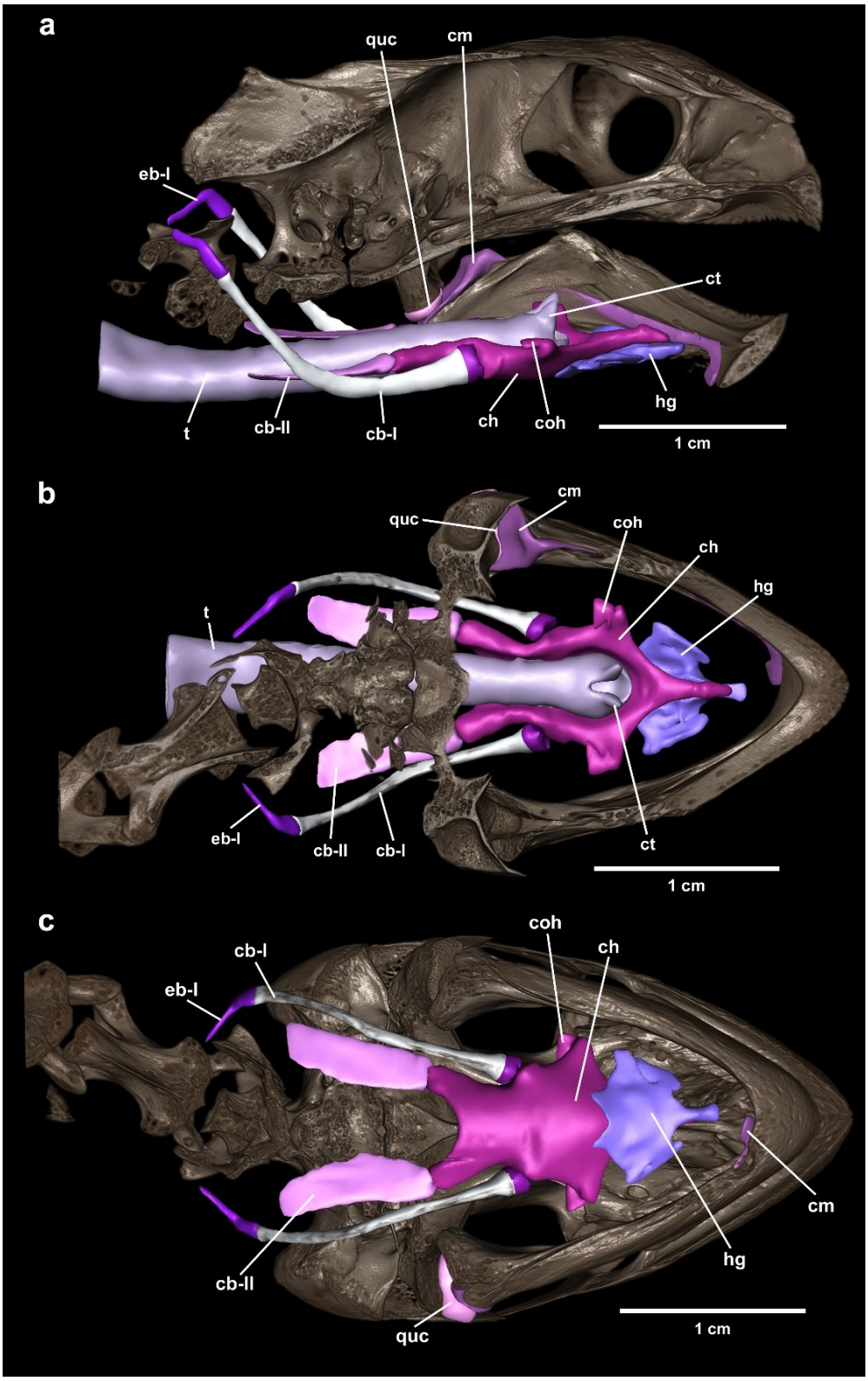

Fig. 5. 3D visualisation of the hyoid complex of *C. mouhotii* based on image segmentation and volume rendering. (a) Medial view of the skull (grey). (b) Dorsal view of the hyoid complex, cut in a frontal axis, only the mandible and part of the quadratum are displayed. (c) Ventral view showing the complete skull, note the broad hypoglossum. Except of the cornu branchiale-I all hyoid bones, as well as the cartilago meckeli and the quadratum cartilage, are cartilaginous. **cb-I**, cornu branchiale-I; **cb-II**, cornu branchiale-II; **ch**, corpus hyoidei; **cm**, cartilago meckeli; **coh**, cornu hyale; **ct**, cartilago thyreoidea; **eb-I**, epibranchiale-I; **hg**, hypoglossum; **quc**, quadratum cartilage; **t**, trachea.

Elements of the lower jaw and the jaw joint

Dental

Almost half of the lower jaw consists of the dental, which builds up the anterior part. Dorsally on the outside it connects to the coronoid, lateromedially with the surangular and ventrally with the angular (Fig. 3). At the side of the oral cavity it is lateromedially in contact with the prearticular, where the cartilago meckeli (Fig. 5) and the nervus maxillaris (N V_2) of the nervus trigeminus (N V) (Figs. 6; 14) leave the lower jaw.

Angular

The angular is placed ventrally in between the articular, which borders it posteriorly, and the dentale (Fig. 3).

Coronoid

At the most dorsal point right in the middle the coronoid is situated (Fig. 3). The main attachment of the coronar aponeurosis is located there.

Surangular

The surangular lies laterodorsally on the posterior part of the lower jaw. It is bordered by the articular posteroventrally, the angular ventrally and the dental anteriorly (Fig. 3). It has a large surface area for the attachment sites of the adductor mandibulae complex.

Preaticular

The counter part to the outside surangular is the prearticular on the inside of the lower jaw (Fig. 3). The adductor mandibulae is predominantly attached to these two bones.

Articular

The most posterior part of the lower jaw is the articular. It is connected to the angular ventrally and the prearticular and surangular anteriorly (Fig. 3). In combination with the cartilago meckeli and the quadratum it builds up the jaw joint.

Cartilago meckeli

This cartilaginous structure defines the ventral, lower jaw part of the jaw joint. It is connected to the articular, the prearticular, the angular and the surangular at the jaw joint, runs rostrad between prearticular and surangular, and exits the lower jaw between prearticular and dental. It then reaches up to the mandible symphysis on the mouth floor. The cartilage at the joint builds a wide groove that elongates dorsally and articulates with the quadratum cartilage (Fig. 5).

Quadratum

The quadratum builds up the biggest part of the otic capsule as well as the cava tympani (Figs. 3; 4). Concerning feeding mechanisms it is of utter importance for the jaw joint. It builds the dorsal part of the joint, where its cartilage articulates with the groove of the cartilago meckeli (Fig. 5). It connects posterodorsally with the squamosal, dorsomedially with the prootic and further posterior with the opisthotic (Figs. 3; 4).

Further bony elements involved in the feeding process

Pterygoid

The U-shaped pterygoid forms a big part of the oral cavity. It builds most of the posterior part of the roof of the mouth. It lies horizontally between the palatine and vomer medioanteriorly and the basisphenoid medioposteriorly (Figs. 3; 4). Laterally it connects to the quadratum and the maxilla. Parts of the floor of the orbital cavity are formed by the pterygoid.

Palatine

Between the maxilla laterally, the vomer medially and the pterygoid posteriorly, the triangular shaped palatine forms a part of the roof of the oral cavity (Figs. 3; 4).

Basisphenoid

The unpaired basisphenoid forms a keel on the roof of the oral cavity between the pterygoid (Figs. 4). On the posterior side it is bordered by the basioccipital. It separates the paired m. adductor mandibulae internus pars pterygoideus posterior from each other medially, on the mouth roof.

Squamosal

The wide posteriorly vaulted squamosal connects to the opisthotic ventromedially and to the quadratum anteriorly (Figs. 3; 4). The otic capsule is shielded by the squamosal to the outside posteriorly.

Opisthotic

Between the squamosal and the exoccipital lies the opisthotic, which is bordered ventrally by the quadratum (Fig. 4). It margins the skull posteriorly. The posterior part of the otic capsule is formed by the opisthotic (Fig.14).

4.1.2 Musculature of the feeding apparatus

The nomenclature follows the one proposed by Werneburg (2011), starting with musculature enervated by nervus trigeminus (N V), because of its strong involvement with the jaw musculature. Numbers of the muscle portions according to Werneburg (2011) are mentioned in parentheses after the muscle's names. The central nervous system was reconstructed (Fig. 6) to help identify muscles. Some muscle portions were not resolved in this study due to the resolution of the microCT image-stacks. The focus lies on the muscles associated with the feeding apparatus.

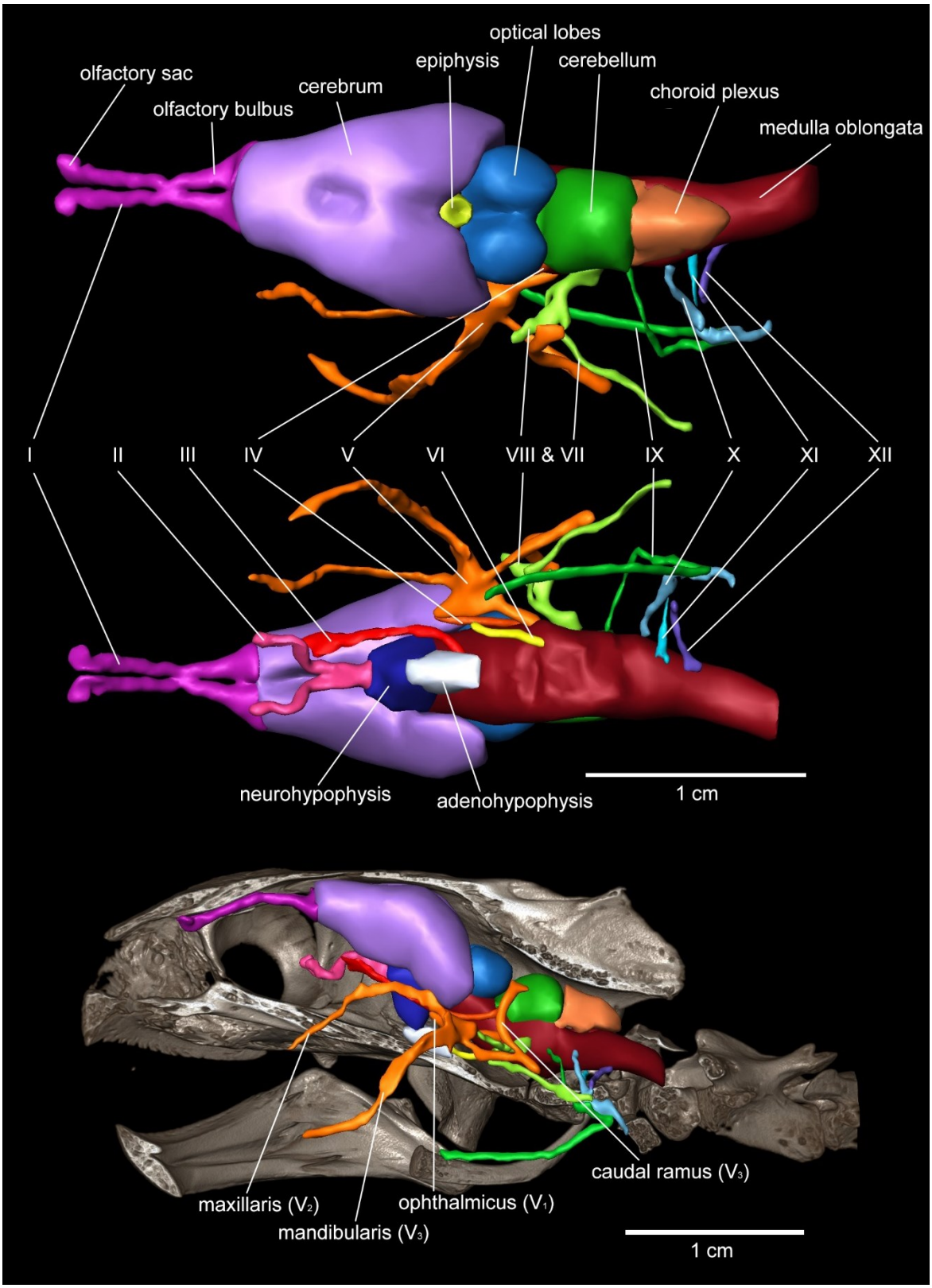

Fig. 6. Central nervous system of *C. mouhotii*, based on 3D visualisation with a volume rendering and segmentation. From top to bottom, the brain is shown dorsally, ventrally and laterally inside the brain capsule. In the latter the segmentation is combined with the volume rendering. The medulla oblongata was only partly reconstructed caudad. All twelve brain nerves are shown. Mostly, just their starting point was identifiable. **I**, nervus olfactorius; **II**, nervus opticus; **III**, nervus oculomotorius; **IV**, nervus trochlearis; **V**, nervus trigeminus; **VI**, nervus abducens; **VII**, nervus facilis; **VIII**, nervus vestibulocochlearis; **IX**, nervus glossopharyngeus; **X**, nervus vagus; **XI**, nervus accessorius; **XII**, nervus hypoglossus.

Musculature innervated by nervus trigeminus V

M. adductor mandibulae externus (m.add.man.ext.)

This muscle describes the lateral part of the adductor mandibulae muscles. It is not the most complex part regarding its different portions, but has the biggest muscle volume of the adductor muscles. Two portions are found, m.add.man.ext. pars profundus (19) (amepp) on the inside and m.add.man.ext. pars superficialis (21) (ameps) laterally (Figs. 7; 9; 14). In between they are divided by the coronar aponeurosis (Figs. 7; 8; 9a). Its insertion area reaches over three bones of the lower jaw, anteriorly the dental, mediodorsally the coronoid and posteriorly the surangular. Some parts of this tendon reach between the lower jaw and the rhamphotheca and seem to connect to the most posterior part of the rhamphotheca. From the dorsal posterior part of the skull the coronar aponeurosis runs ventrally to the coronoid of the lower jaw. The tendon builds a flattened surface in the vertical axis. It bends horizontally over the quadratum and reaches far back into the muscle, where it gradually decreases in diameter (Fig. 8). At this bend, the tendon thickens and builds a smooth surface against the cartilaginous tissue of the anterior quadratum and prootic, namely the trochlear process. This thin cartilage layer builds up a gliding surface for the coronar aponeurosis, at which it can slide back and forth. The structure of the coronar aponeurosis does not indicate a cartilago transiliens, but it is thickened at that point. It provides amepp and ameps with an insertion point on its lateral and its median side. Furthermore, a broad insertion area of the ameps spans between the lateroposterior part of the dental, the coronoid and the surangular. The most dorsorostral part of the muscle merely attaches with some fibres at the dorsal part of the postorbital. Both amepp and ameps originate from the parietal, the supraoccipital, and further caudal at the supraoccipital fascia, where they attach in a pinnate form. In the most posterior part, although they are marked as separate muscles, they fuse together. The origin of the coronar aponoeurosis marks the rostral beginning of the separation of these muscle portions. Amepp attaches to the coronar aponeurosis on the inside and originates on the inner part of the parietal. It reaches posterior, where it is attached to the skull and on a fascia caudally of the supraoccipital. Both muscles are innervated by the N V. Specifically the ramus caudalis of the nervus mandibularis (N V_3) reaches into the ventral posterior part of the amepp (Figs. 6; 9; 13; 14).

A m.add.man.ext. pars medialis (17) (amepm) was not clearly distinguishable and therefore included in the segmentation of the ameps (21). Some fibres, which were only identifiable in the dissection, run from the ventral part of the quadratum rostrally to the coronar aponeurosis and insert into the fibres of the ameps.

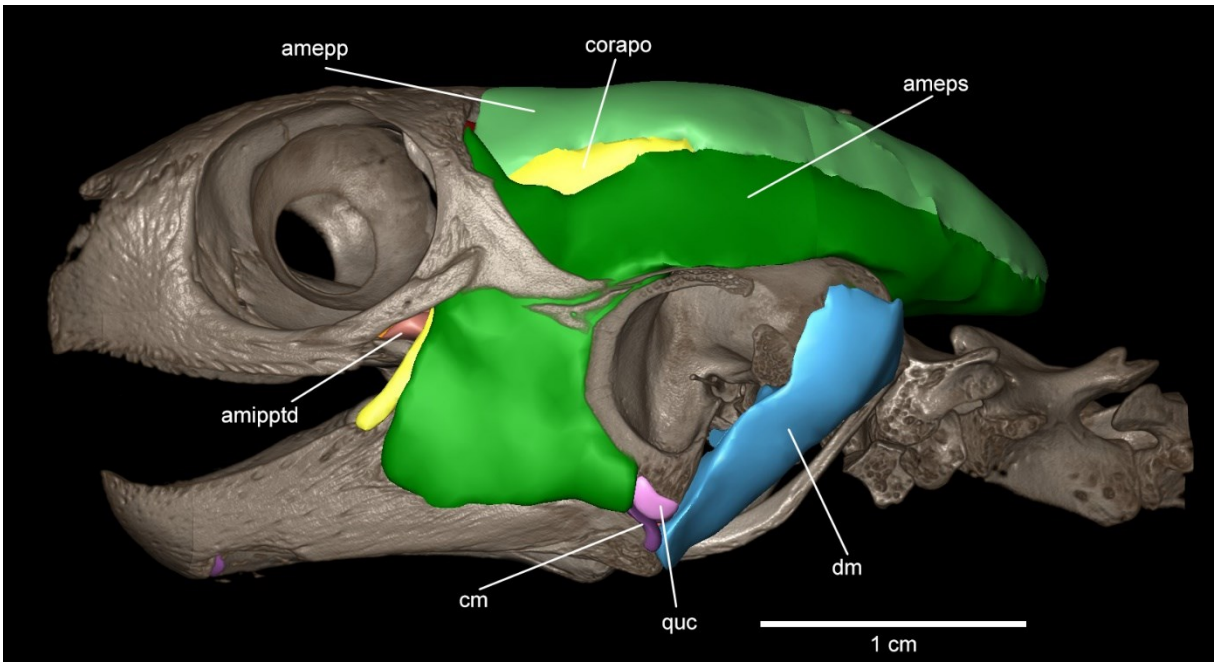

Fig. 7. Lateral view of the skulls 3D visualisation of *C. mouhotii* with the adductor mandibulae externus (green), the coronar aponeurosis (yellow) and the depressor mandibulae (blue) shown. The add.man.externus spans far posterior even further than the supraoccipital. In the last third the amepp and the ameps were not distinguishable, therefore they were separated into two equal parts, even though they both share the same origin posteriorly. **amepp**, m. add.man.ext. pars profundus; **ameps**, m. add.man.ext. pars superficialis; **amipptd**, m.add.man.int. pars pterygoideus dorsalis; **cm**, cartilago meckeli; **corapo**, coronar aponeurosis; **dm**, depressor mandibulae; **quc**, quadratum cartilage.

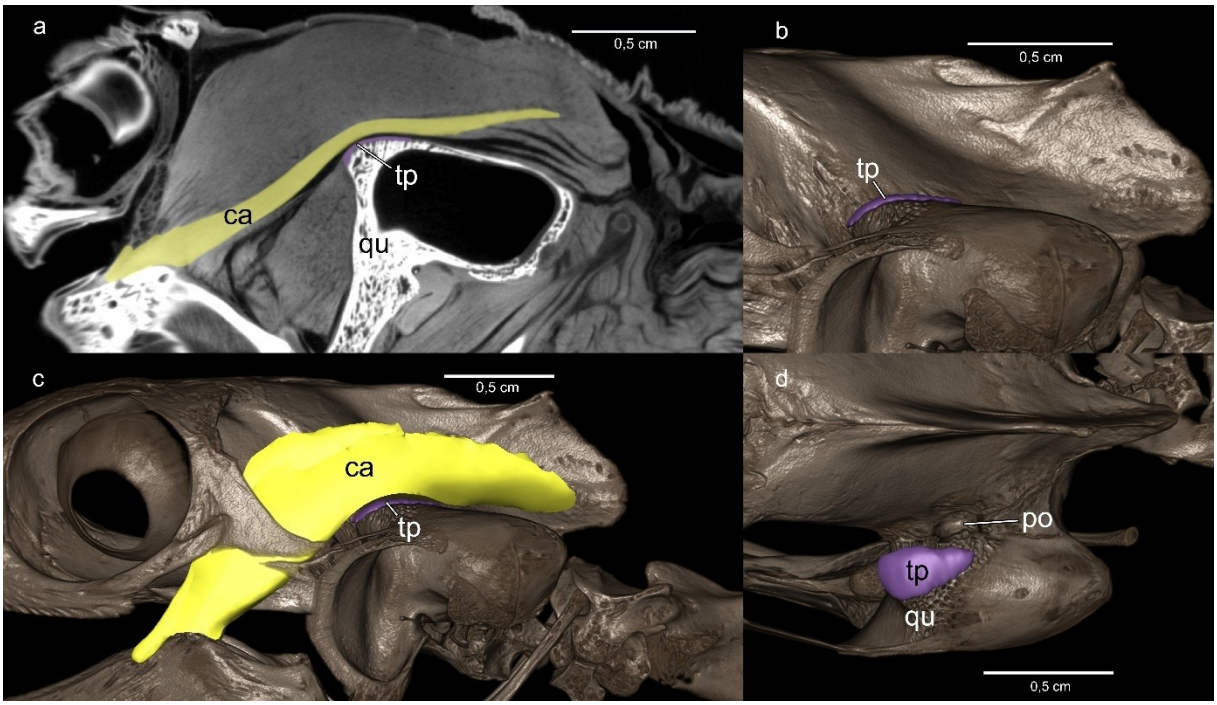

Fig. 8. 3D visualisation based on segmentation and volume rendering of *C. mouhotii*. Lateral and dorsal views of the trochlear process, which builds up a gliding surface with the coronar aponeurosis. The coronar aponeurosis slides over the cartilage, transferring its horizontal pulling force into a more vertical one. (a) Lateral picture of the microCT ethanol fraction, the coronar aponeurosis is marked in yellow; (b) Lateral view, showing the trochlear process on the quadratum; (c) lateral view of the coronar aponeurosis and its gliding surface; (d) dorsal view of the trochlear process. **ca**, coronar aponeurosis; **po**, prootic; **qu**, quadratum; **tp**, trochlear process.

M. adductor mandibulae internus (m.add.man.int.)

The following muscles are described in order of their origin from dorsally to ventrally. Both the m.add.man.int. pars pseudotemporalis (23) (amipps) as well as the m.add.man.int. pars pseudotemporalis superficialis (24) (amippss) have their origin on the skull roof at the ventral part of the parietal roof, rostrad to the attachment of the ameps (21). The latter, amippss (24) is situated lateral to the amipps. They are hard to separate in the microCT stack since the muscle fibres are often weaved into each other especially ventrally. The mandibular nerve (V_2) splits them apart in the upper half of the muscle (Fig. 9). Directly rostral of the maxillomandibular ganglion (Fig. 13) the nerve enters those muscles. The amippss is laterally circled by the (V_3), which runs further anteroventrally and enters the lower jaw. Both muscles spanning dorsoventrally attach at different small sites to the prearticular.

In-between the m.add.man.int. a big aponeurosis is situated (Fig. 10). It lies ventrally and reaches from the articular and foremost the prearticular dorsorostrad. It is composed of more than one aponeurosis, which build up an indistinguishable complex like the m.add.man.int. does at the most ventral third. For consistency reasons, this aponeurosis cannot be resolved with certainty and therefore is called adductor mandibulae internus aponeurosis (intapo) in this thesis, which is in the nomenclature of Werneburg (2011) only a part of an aponeurosis complex.

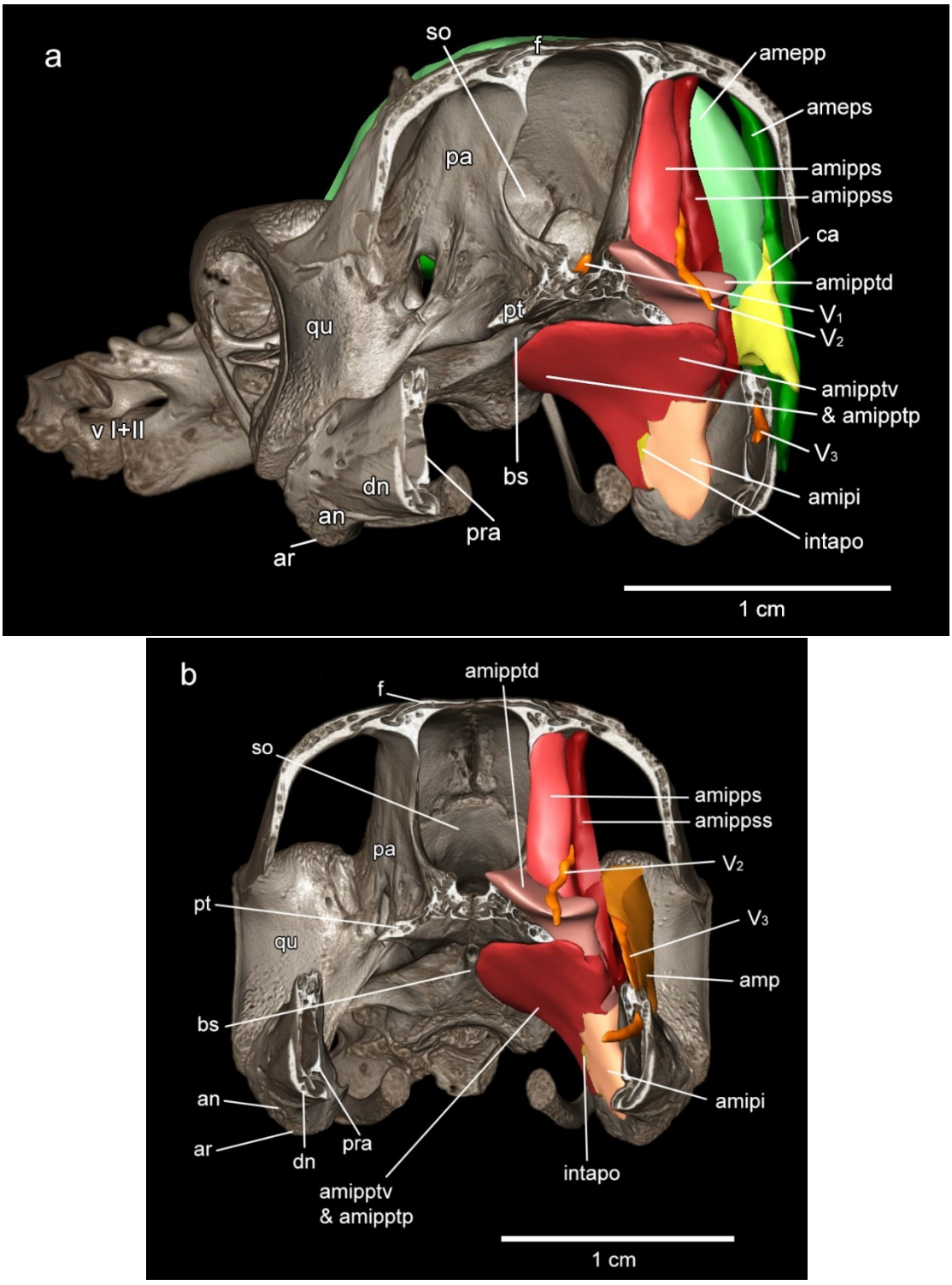

Fig. 9. 3D visualisation of *C. mouhotii* combining volume rendering and segmentation. In both images a transverse cut, in the region of the posterior mandible, was carried out. Displayed in colour is the segmentation of the adductor mandibulae complex corresponding to nervus trigeminus V (orange). (a) The view axis is rotated a bit to the side. The adductor mandibulae externus (green), the coronar aponeurosis (yellow) and the adductor mandibulae internus (red) are displayed. (b) frontal view; note that the m.add.man.ext. as well as the coronar aponeurosis were removed. **amepp**, m.add.man.ext. pars profundus; **ameps**, m.add.man.ext. pars superficialis; **amipi**, m.add.man.int. pars intramandibularis; **amipps**, m.add.man.int. pars pseudotemporalis; **amippss**, m.add.man.int. pars pseudotemporalis superficialis; **amipptd**, m.add.man.int. pars pterygoideus dorsalis; **amipptp**, m.add.man.int. pars pterygoideus posterior; **amipptv**, m.add.man.int. pars pterygoideus ventralis; **amp**, m.add.posterior; **an**, angular; **ar**, articular; **bs**, basisphenoid; **dn**, dental; **f**, frontal; **intapo**, internus aponeurosis; **pa**, parietal; **pra**, prearticular; **pt**, pterygoid; **qu**, quadratum; **so**, supraoccipital; **V1**, nervus ophtalmicus; **V2**, nervus maxillaris; **V3**, nervus mandibularis.

On the dorsal side of the pterygoid the m.add.man.int. pars pterygoideus dorsalis (26) (amipptd) has its origin. Rostrad it is flattened, the fibres twist and reach posteroventrally underneath the pterygoid to the mouth cavity, where they combine with fibres of the m.add.man.int. pars pterygoideus posterior (27) (amipptp) and ventralis (28) (amipptv) and the m.add.man.int. pars intramandibularis (25) (amipi). In the ventral two thirds they are separated by the intapo. In this part of the mandible internus muscle complex the fibres cannot be clearly separated and therefore the borders in this section of the reconstruction should not be seen as clear lines where one muscle ends and the other starts, but rather as loose boundaries where muscle portions merge together. The amipptp and the amipptv were indistinguishable and describe the posterior and ventral parts of the internal mandibular muscles attaching directly to the pterygoid. The basioccipital represents the boundary in the middle of the roof of the mouth for these muscles. They attach to the mandible at the articular and the intapo (Fig. 10). The smallest portion of the m.add.man.int. (ami), which lies directly at the prearticular, is the amipi (25). It connects to the intapo, amipps and amippss and dorsally merges together with amipptd, amipptp and amippts. Together, m.add.man.ext. (ame) and ami are responsible for the jaw closing (Fig. 12)

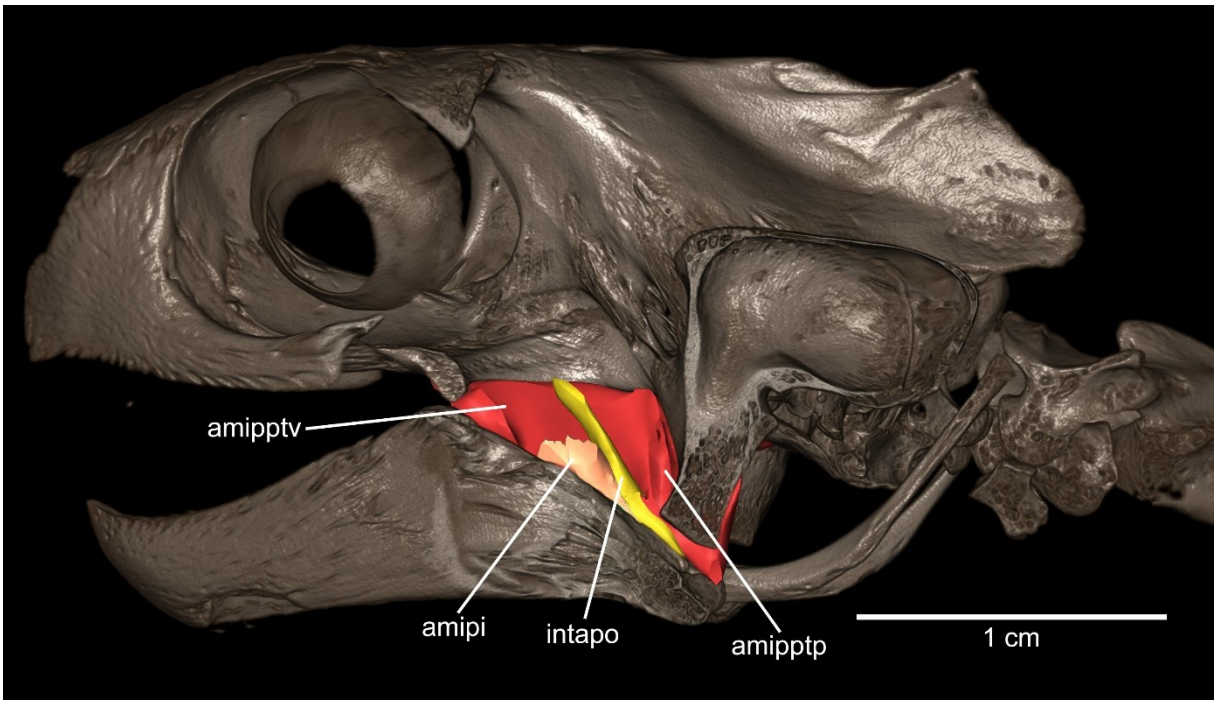

Fig. 10. Lateral view of the 3D visualisation of *C. mouhotii.* A lateral sagittal virtual cut was done to remove the surangular in the mandible, as well as parts of the quadratum laterally, the whole postorbital, jugal and quadratojugal. Note the internus aponeurosis in-between the amipptv and the amipptp, above the amipi. To get a clear lateral view of this aponeurosis, situated in the middle of the m.add.man.int. muscle complex, the m.add.man.ext., the coronar aponeurosis, the amipptd as well as both amipps where removed. **amipi**, m.add.man.int. pars intramandibularis; **amipptp**, add.man.int. pars pterygoideus posterior; **amipptv**, add.man.int. pars pterygoideus ventralis; **intapo**, internus aponeurosis.

M. adductor mandibulae (m.add.mand.) posterior

The m.add.mand. posterior (29) (amp) spans dorsoventrally. It reaches to the mandible and inserts mostly to the cartilago meckeli, but also to the intapo. These fibres are in close proximity to the amippt (26), (27) and (28) and seem to transition into each other. The amp has its origin at the groove between parietal and quadratum dorsomedially. It is situated posterior to the ami. Laterally it is bordered by the amepp, and medially by the maxillomandibular ganglion (Figs. 9; 13). The anterior part of the amp is in close proximity to the amipptd, which appear to fuse together at one point (Fig. 11).

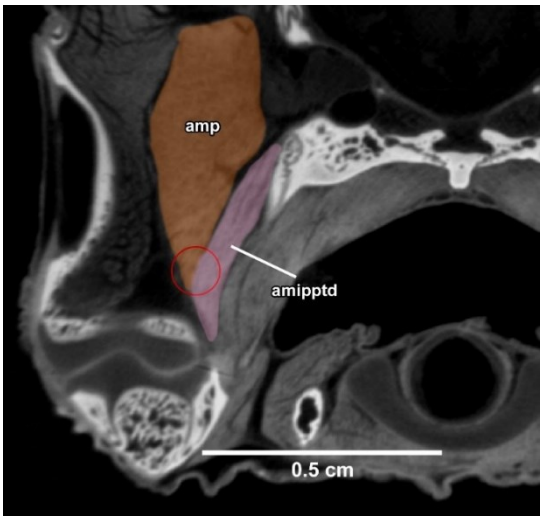

Fig. 11. Selected is a microCT slice of the posterior part of the mouth cavity, at the level of the jaw joint, of *C. mouhotii*. The red circle indicates, where **amipptd**, m.add.man.int. pars pterygoideus dorsalis (pink), and **amp**, m. adductor mandibulae posterior (brown), meet and transition into each other.

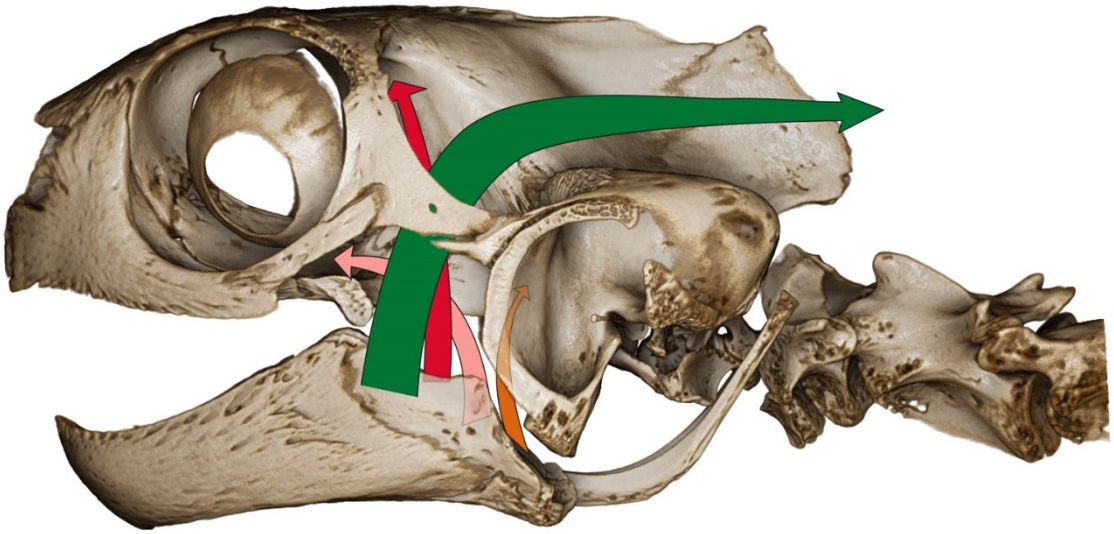

Fig. 12. Depicted is a 3D visualisation of *C. mouhotii* with all mandible adductor muscle force vectors displayed in the same colour as in the figures. Illustrated are the forces generated on the lower jaw, when closing the mouth. The thickness of the arrows shows the estimated force created by these muscles, judged by their volume and their diameter, following Lemell et al. (2000). **Green**, m.add.man.ext. pars profundus and pars superficialis; **red**, m.add.man.int. pars pseudotemporalis and pars pseudotemporalis superficialis; **rose**, m.ad.man.int. pars pterygoideus dorsalis and pars pterygoideus posterior and pars pterygoideus ventralis; **orange**, m.add.man. posterior.

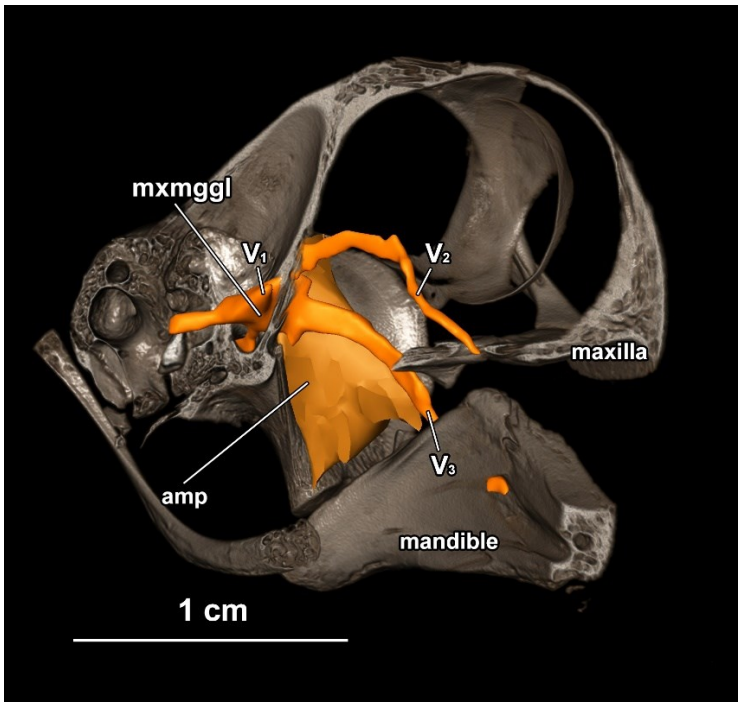

Fig. 13. Virtual sagittal section through the volume rendered skull of *C. mouhotii*. The viewpoint is from laterofrontal, to give a better visibility to the amp. The mandible is on the lower right. On the upper right, the digital cut goes through the maxilla and the orbital cavity in which the ossified parts of the eye bulb are visible. The posterior part shows the otic region. Nervus trigeminus is included as well, which nestles into the median side of the amp. Further all the three major branches of the N V (V_1; V_2; V_3) are clearly recognizable. No fibres of the muscle attach directly to the bones of the lower jaw. Some fibres insert at the intapo, but most of them at the cartilago meckeli. **amp**, m. adductor mandibulae posterior; **mxmggl**, maxillomandibular ganglion; **V_1**, nervus ophthalmicus; **V_2**, nervus maxillaris; **V_3**, nervus mandibularis.

M. intermandibularis (im)

The im (31) (Fig. 15), as its name suggests, is located between both dentals and angulars. The fibres of this flat muscle stretch from their attachment site on the lower jaw to a median raphe. It shows a U-shape in cross section, at which the lateral parts are thicker than the flat parts medially. This muscle is innervated by the N V_3. It builds the most ventral part of the mouth floor and stretches anterior close to the tip of the lower jaw and posterior up to the end of the angular.

Musculature innervated by nervus facialis VII

M. constrictor colli (42) is divided into different portions, which could not resolved. Posterior it lies ventral to the m. intermandibularis (Fig. 15). It reaches to the median raphe ventral of the trachea and runs further posterior. The fibres going posterior split into a ventral and a dorsal part and build up the outmost muscle layer of the turtle's neck.

Two other muscles, m. depressor mandibulae (dm) (45) and m. dilitator tubae (dt) (46) were at least at their ventral attachment completely undistinguishable. Going ventral the fibres merge

together. Dm is located more to the outside, whereas dt originates more medial. Dm is attached to the posterior side of the articular (Fig. 7) and the cartilago meckeli. Its origin is at the posterior side of the squamosal (Fig. 14) as well as the cartilaginous structure of the tuba eustachii.

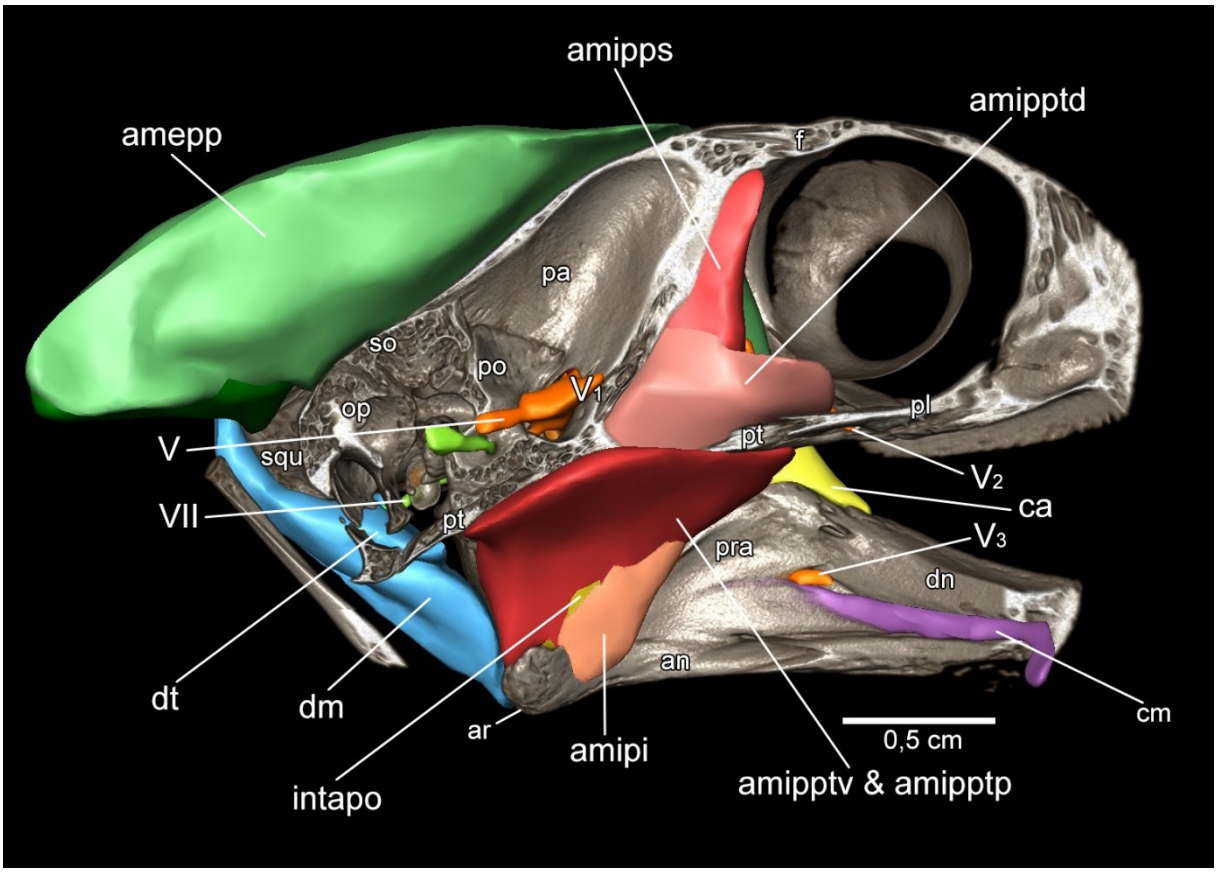

Fig. 14. Displayed is a 3D visualisation of *C. mouhotii* based on a volume rendering combined with a segmentation. This sagittal section runs through the otic capsule. The segmentation shows the m.add.man.ext., the m.add.man.int. and the dm. Note also the two nerves innervating these muscles: N VII runs posteroventrally to the dm and dt, and the N V runs anterior and splits into three parts. **amepp**, m.add.man.ext. pars profundus; **amipi**, m.add.man.int. pars intramandibularis; **amipps**., m.add.man.int. pars pseudotemporalis; **amipptd**, m.add.man.int. pars pterygoideus dorsalis; **amipptp**, m.add.man.int. pars pterygoideus posterior; **amipptv**, m.add.man.int. pars pterygoideus ventralis; **an**, angular; **ar**, articular; **ca**, coronar aponeurosis; **dm**, depressor mandibulae; **dn**, dental; **dt**, dilatator tubae; **f**, frontal; **op**, opisthotic; **pa**, parietal; **pra**, prearticular; **pl**, palatine; **po**, postorbital; **pt**, pterygoid; **so**, supraoccipital; **squ**, squamosal; **V1**, nervus ophtalmicus; **V2**, nervus maxillaris; **V3**, nervus mandibularis.

Musculature innervated by nervus glossopharyngeus IX

M. branchiomandibularis visceralis (47) (bm) is innervated by nervus glossopharyngeus IX (N IX), which runs lateromedially to the muscle and reaches forward into the tongue. The muscle attaches at the most posterior part of cb-I and partly on the eb-I and runs anteroventrally and originates at the lower jaw at the angular and prearticular (Fig. 15).

Musculature innervated by nervus hypoglossus XII

Rostral to the origin of the bm (47) the anterior part of the cb-I is covered by the origin of the m. branchiohyoideus (55) (bh). It inserts ventrally and posterior at the cornu hyale as well as the ventral side of the corpus hyoidei (Fig. 15). This muscle and the following three are innervated by the nervus hypoglossus XII (N XII), of which the origin at the medulla oblongata was reconstructed (Fig. 6).

M. coracohyoideus (58) (co) starts at the coracoid, although it was not seen in the microCT scan, because the head was cut anterior of the coracoid. The muscle reaches ventrally and attaches to the trachea at the median raphe, the corpus hyoidei and the cb-II (Fig. 15).

M. genioglossus (63) (gg) originates at the mandible symphysis, reaches lateral and attaches to the hypoglossum ventrally. Dorsally the muscle is appended to the tongue with thick connective tissue surrounding the muscle fibres (Fig.15).

M. geniohyoideus (64) (gh) originates at the medial anterior part of the cb-I (Fig. 15). The fibres run rostrad between the m. intermandibularis and the corpus hyoidei. Its anterior insertion lies ventrally on the hypoglossum, in close proximity to the gg.

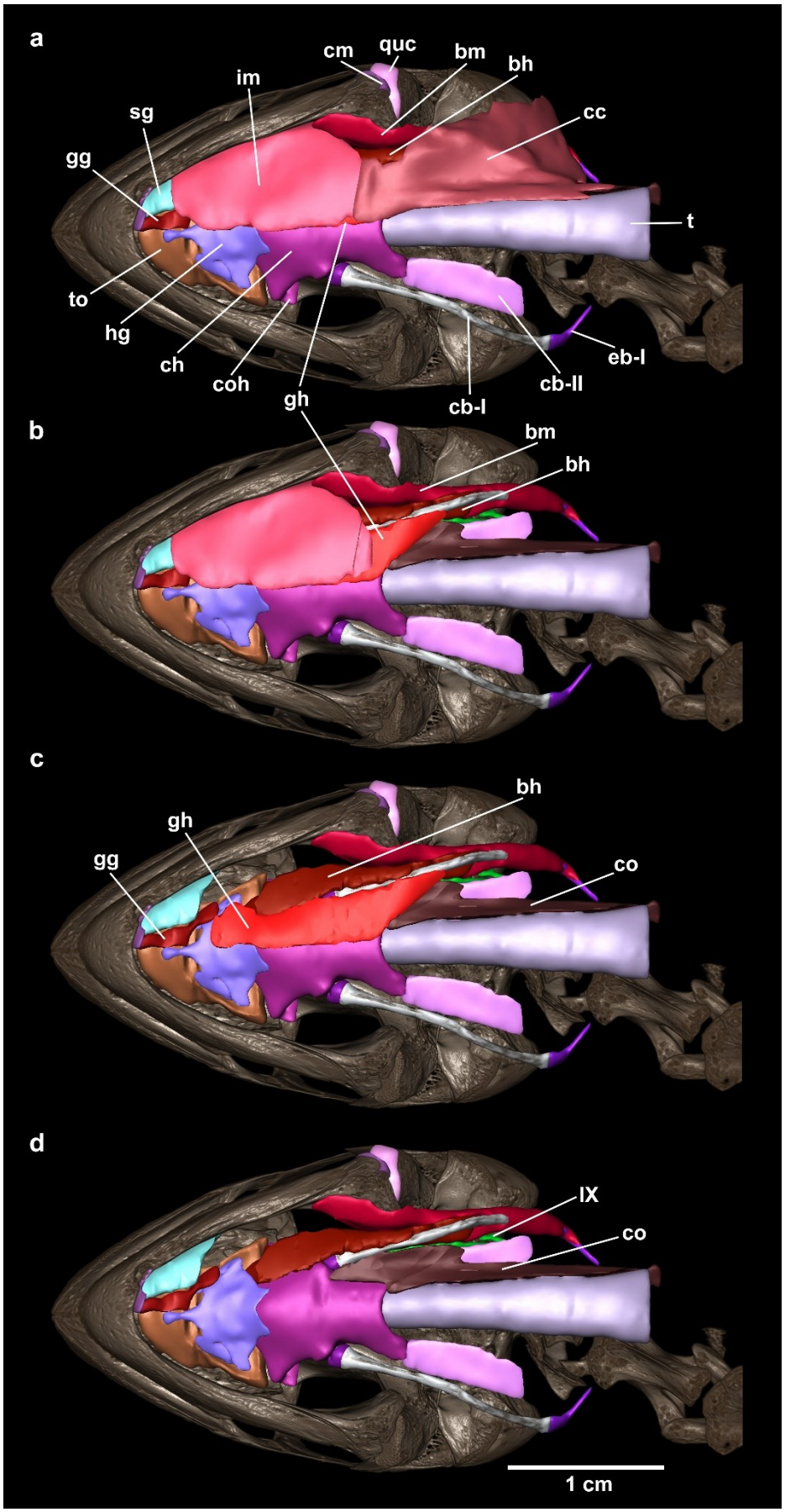

Fig. 15. Ventral view of the 3D visualisation of the skull of *C. mouhotii* (grey) with segmentation of the hyoid apparatus and its musculature (a). From top to bottom, different muscles are removed to reveal the muscle beneath. In (b) m. constrictor colli is removed, followed by (c) m. intermandibularis. In (d) m. geniohyoideus was removed. Note that m. coracohyoideus and m. constrictor colli are partly attached to the trachea. **an**, angular; **ar**, articular; **bh**, m. branchiohyoideus; **bm**, m. branchiomandibularis; **cb-I**, cornu branchiale-I; **cb-II**, cornu branchiale-II; **cc**, m. constrictor colli; **ch**, corpus hoyidei; **cm**, cartilago meckeli; **co**, m. coraco-hyoideus; **coh**, cornu hyale; **quc,** quadratum cartilage; **dn**, dental; **gg**, m. genioglossus; **gh**, m. genio-hyoideus; **hg**, hypoglossum; **im**, m. intermandibularis; **pra**, prearticular; **sg**, salivary gland; **t**, trachea; **to**, tongue; **IX**, nervus glosso-pharyngeus.

4.1.3. Muscles and nerves associated with the eye

Musculature innervated by nervus oculomotorius III

M. obliquus inferior (oblinf) has its insertion on the ventral part of the eye bulbus. It reaches rostral were it has its origin partly on the septum orbitalis, which separates the optic cavities. Dorsally of the insertion site of oblinf lies the m. rectus anterior (2) (recant). Its insertion is broad and the fibres run posterior where its origin lies anteriorly to the foramen opticum. Ventrally of the recant the m. rectus inferior (3) (recinf) reaches ventrorostrad to the ventral part of the eye. M. rectus superior (4) (recsup) is situated dorsally to the foramen opticum and has its insertion further dorsal at the eye. All four described muscle are innervated by the nervus oculomotorius (N III), which lies dorsally of the m. retractor bulbi (38) (retbulbi) (Fig. 16).

Musculature innervated by trochlearis IV

Innervated by the n. trochlearis (N IV) is the m. obliquus superior (9) (oblsup). Of all eye muscles it is the most anterior one and originates dorsoanteriorly of the oblinf. It then reaches further dorsal and posterior on the dorsal part of the eye. The insertion is broad and lessens in width compared to its origin (Fig. 16).

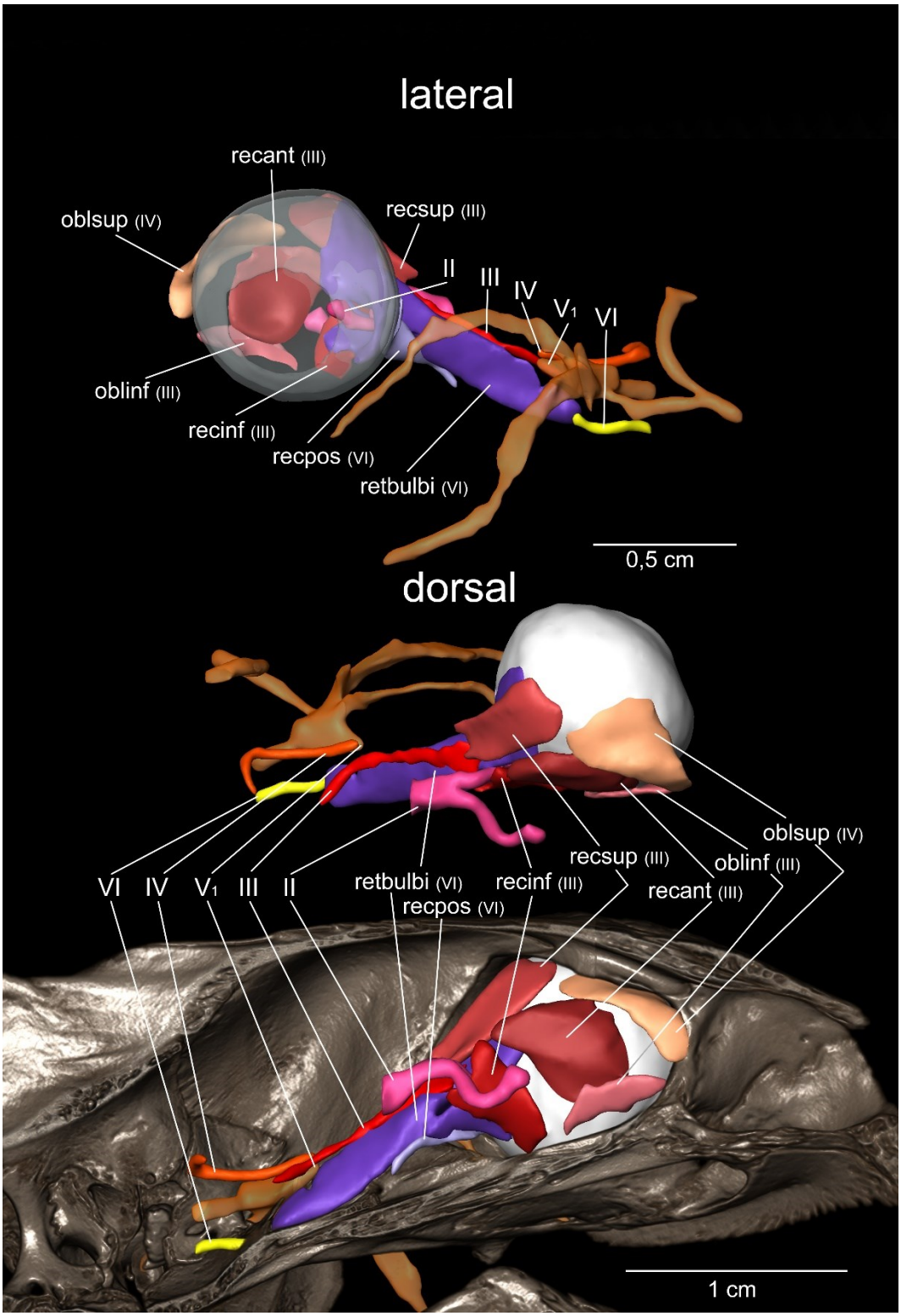

Fig. 16. The morphology of the eye, corresponding eye muscles and their innervation are displayed based on 3D visualisation methods of a volume rendering and segmentation. The eye bulbus is white transparent on the top picture, to see the attachment sites of the eye muscles. **N**ervus opticus is fully reconstructed, other nerves are only partly visualized. The longer parts of nervus trigeminus, like the **V_2**, the **V_3** and the caudal ramus are not involved in the innervation of the eye muscles. Only the origin is reconstructed of the nervus ophthalmicus **V_1**. The image at the bottom displays a sagittal cut through the skull, viewed medially. **oblinf**, m. obliquus inferior; **oblsup**, m. obliquus superior; **recant**, m. rectus anterior; **recinf**, m. rectus inferior; **recpos**, m. rectus posterior; **recsup**, m. rectus superior; **retbulbi**, m. retractor bulbi; **II**, nervus opticus; **III**, nervus oculomotorius; **IV**, nervus trochlearis; **V**, nervus trigeminus; **VI** nervus abducens.

Musculature innervated by nervus abducens VI

M. rectus posterior (37) (recpos) is another eye rotating muscle found in *C. mouhotii*. Ventrally of the prominent retbulbi the fibres of recpos run dorsorostrad, switch underneath the retbulbi to the lateral side and insert at the lateral posterior part of the eye. The thickest of the eye muscle is the retbulbi which inserts in a groove of the basisphenoid and runs dorsorostral. It widens and splits into two parts which surround the nervus opticus (N II). The greater part inserts above the N II at the posterior median part of the eye bulbus.

Musculature innervated by cervical nerves

M. carapacocervico-capitis lateralis pars capitis (81) (cal) and m. carapacocervico-capitis medialis pars capitis (82) (cam). These muscles have their origin at different vertebrae, foremost the first three. They run rostrad and cover the posterior part of the amepp (19) and ameps (21) (Fig.17).

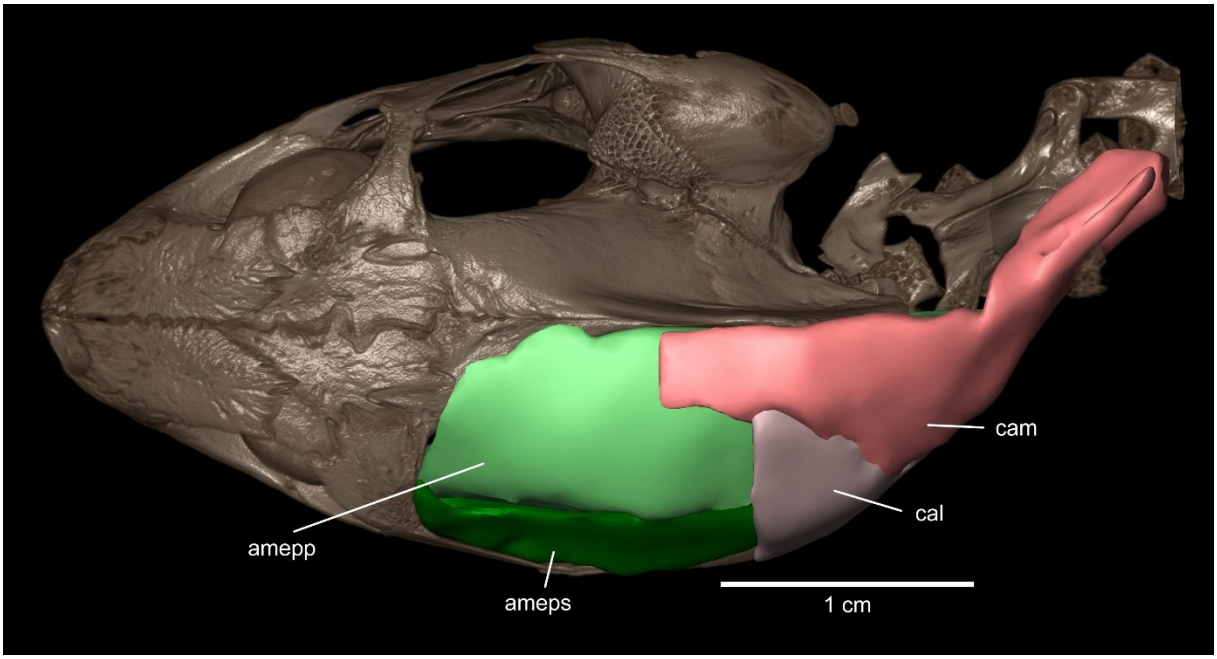

Fig. 17. Dorsal 3D visualisation of *C. mouhotii* showing the m.add.man.ext., which is in its posterior part covered by the two muscles, m. carapacocervico-capitis lateralis pars capitis and m. carapacocervico-capitis medialis pars capitis. The latter has its origin at the first three vertebrae, so the origin is not completely visible in this image. **amepp**, m.add.man.ext. pars profundus; **ameps**, m.add.man.ext. pars superficialis; **cal**, m. carapacocervico-capitis lateralis pars capitis; **cam**, m. carapacocervico-capitis medialis pars capitis.

4.1.4. Other morphological features

Rhamphotheca

The rhamphotheca or the horny sheath of the jaws are well developed and thick. Especially at the most anterior part, where they build an acuminate beak, most prominent in the lower jaw (Figs. 18; 19).

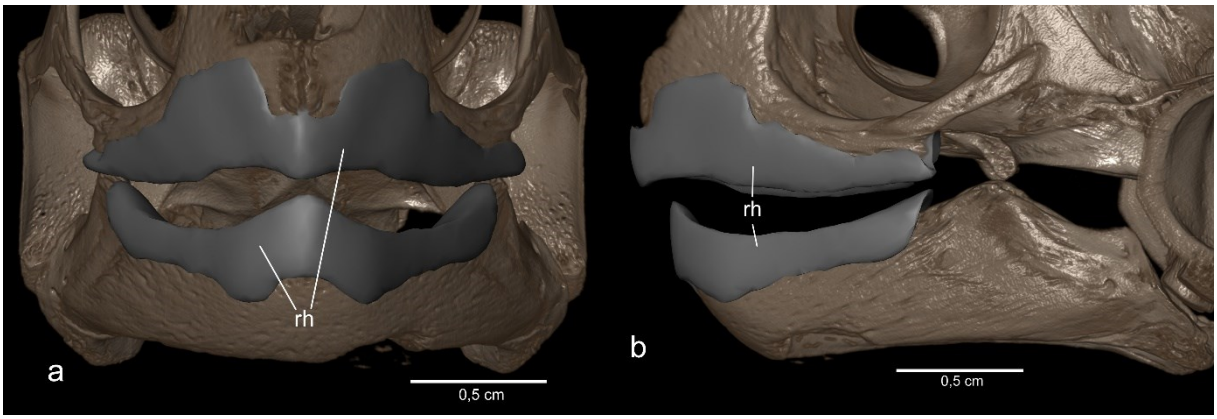

Fig. 18. 3D visualisation of *C. mouhotii* and its rhamphotheca. This horny sheath is built massively on both jaws. (a) frontal view (b) lateral view. Note the sharpness especially of the lower jaw. **rh**, rhamphotheca.

The roof of the mouth has a slight ridge medially, posterior to the rhamphotheca and anteriorly on the vomer. This ridge is followed posteriorly by a groove which is partly build up, but also separated by the vomer in the middle (Fig. 19). The groove of the palate as well as the ridge of the vomer are the two features were the food is pressed against during the feeding cycle.

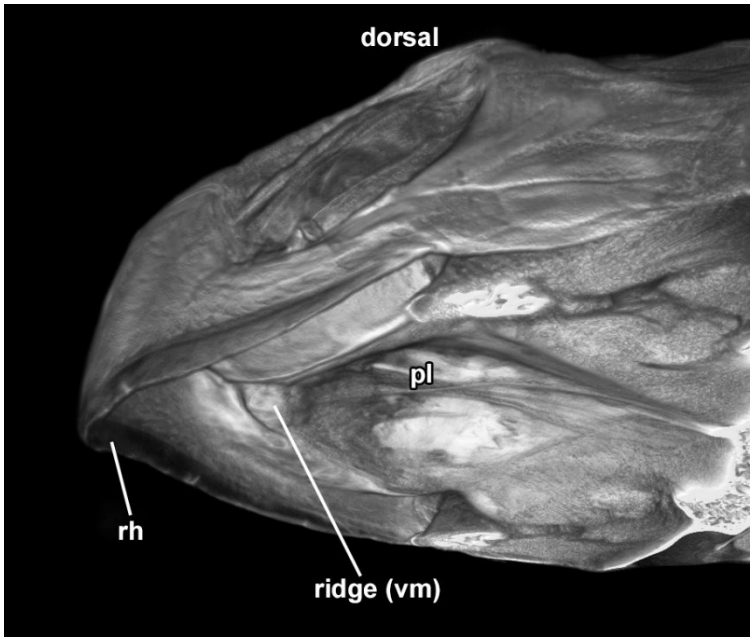

Fig. 19. This 3D visulation is based on a volume rendering and shows the thick rhamphotheca of the upper jaws of *C. mouhotii*. The palate is viewed from lateroventral. A virtual cut was carried out on most dorsal third of the lower jaw. The ridge is built up by the vomer. **pl**, palatine; **rh**, rhamphotheca; **vm**, vomer.

4.1.5. Tongue

The tongue is fleshy and muscular. Anterior of the glottis thick long papillae are visible, which are spread over the triangle shaped tongue (Fig. 20).

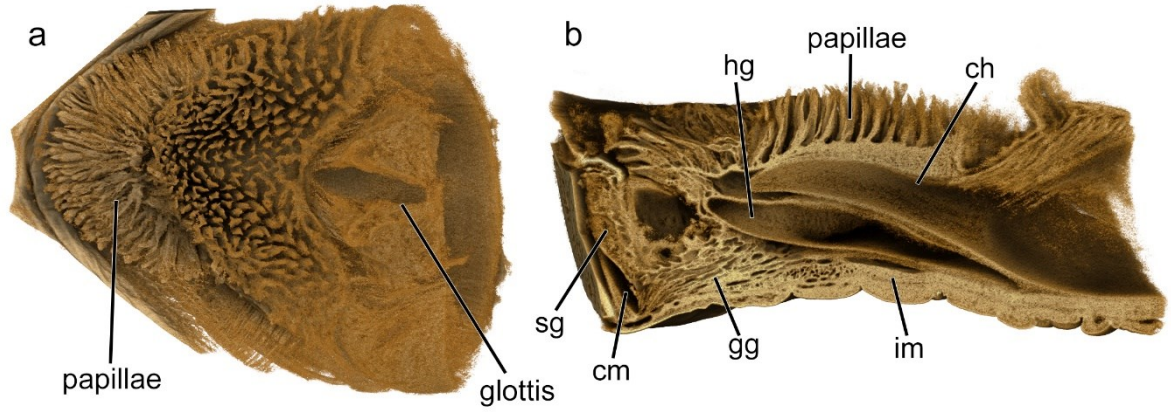

Fig. 20. Volume rendering of the tongue of *C. mouhotii*. (a) Dorsal view of the tongue and its papillae, both mandibles are partly removed. A transverse cut was carried out posterior to the glottis. (b) Lateral sagittal cut in the middle of the mouth floor. Note the long papillae of the tongue. **ch**, corpus hyoidei; **cm**, cartilago meckeli; **gg**, m. genioglossus; **hg**, hypoglossum; **im**, m. intermandibularis; **sg,** salivary gland

4.2. Videography, feeding behaviour and kinematics

4.2.1. Terrestrial feeding

For terrestrial food uptake 28 videos were analysed. In general, not all videos were suitable for analysing manipulation or transport phases due to rotary movement of the head and other complications. Less than half of the videos recorded were analysed. Criteria for further analyses were, that the process of food uptake was clearly visible from a lateral view and the ingestion had to be fulfilled in one try. Films where multiple tries were needed were not included. When the snails were too big, the turtles required more than one uptake of the snail, which then could not be measured due to inconsistency reasons.

Ingestion is the intake of the food by the jaws, into the oral cavity. This first phase of the feeding cycle consists of an opening and a closing of the jaws. During closing a power stroke can appear, which mostly occurs when feeding on hard prey. It arises as a small bump within the feeding cycle graphs of the jaw. Individual films of the hard food ingestion display no SO phase. However, when averaged, the graph displays a SO due to the high variation in the duration of the mouth opening of the individual films (Fig. 21). After comparing average graphs and individual film graphs it was concluded that the ingestion does not show a SO phase. During ingestion the tongue has a posterior position between the lower jaw, its movement during this

phase is marginal. The ingestion can either be followed by a manipulation phase (MP), in which the animal break up the food, or a transport phase (TP), where the food is transported through the oral cavity. The MP only occurs when necessary and is characterized by an opening of the jaws and a closing, both not further subdivided. This phase is variable due to differences in food properties and the position of food items within the oral cavity. Tongue movement corresponds to the food item. Variable movements are possible, but the tongue movement never has a plateau phase and does not reach the same position as seen in a typical TP. Discrimination of the TP and MP is possible with its corresponding tongue movement and the maximum gape during these phases. MP graphs show a smaller peak in maximum gape than during the TP. In the TP, the tongue reaches rostral, touches the upper jaw and is protruded outside of the mouth. This position is held shortly resulting in a tongue plateau phase. During the TP the prey is pressed against the roof of the mouth by the tongue. Simultaneously the tongue slides anterior, underneath the food, to position it further posterior on the tongue. The pressure against the mouth roof is released during jaw opening when the tongue protracts. Adhesive forces between the tongue and the food item separate the contact of the palate to the food. In contrast, during the MP contact of the tongue to the upper jaw is not existent or the tongue is not held at the same position. TP is split into a slow opening (SO), a fast opening (FO), and a uniform closing phase. MP as well as TP are cyclic, often resulting in more than one cycle until swallowing is possible.

26 videos were used for the ingestion, TP was analysed in 28 videos and MP in 13 videos. Of each video, if possible, two TP and two MP were used, overall resulting in 56 TP cycles and 21 MP cycles. In general, all three individuals preferred snails to fruits. Furthermore, my observation during feeding led me to the conclusion that they differentiated between carnivorous and herbivorous food presented and subsequently they appeared to alter their approaching speed.

The feeding mechanism did always follow the same scheme. The prey was approached at varying speeds and the jaws were slowly opened with a protracted tongue. Following the ingestion by jaw prehension, snails and pear as food sources were handled differently. Snails did require more MP cycles before transport than the soft pears. The occurrence of the MP differed, being more than twice the amount when feeding on hard food (1,93 per film) than on soft food (0,82 per film). With pears the MP were not that common and only occurred in 4 of the 11 pear films. Mean values of the amount of TP resulted in 4,64 per film with soft food and 6,2 per film in hard food.

Ingestion started with the approach toward the prey by elongating the neck. While opening the

jaws, the head to neck angle became more vertical, and the head reached from above over the prey to grasp it. The maximum head protraction occurred 0,104s ± 0,049 after the maximum gape (MG). After ingestion the neck was retracted to its starting position or often further back close to the carapace. Head movement in regard to the carapace did vary individually. Ingestion differed in speed as well as in the duration between soft and hard food (Fig. 21). The duration of the opening when feeding on soft food (0,969 s) was faster than on hard food (1,333 s). Closing was shorter for hard food (0,176 s) than for soft food (0,438 s). The speed reflects the closing results by doubling the mean velocity of soft food (49,801 mm/s) in hard food (105,864 mm/s). The overall highest velocities were found with hard food, during the closing phase, with a maximum velocity of 272,375 mm/s. Looking at the cycle duration of the ingestion itself, thecycle duration for hard food took just a bit longer (1,592 s) than for soft food (1,376 s) (Tab. 1). When feeding on snails a power stroke was detectable in the closing phase. With this power stroke, which was clearly visible as tension of the ame, the snail was crushed. The ingestion graph shows a uniform increase and afterwards decrease in gape, with a power stroke when feeding on snails (Fig. 21). The maximum gape angles were relatively close with 43,5° ± 4,6° for hard food and 39,9° ± 6,7° for soft food (Fig. 22).

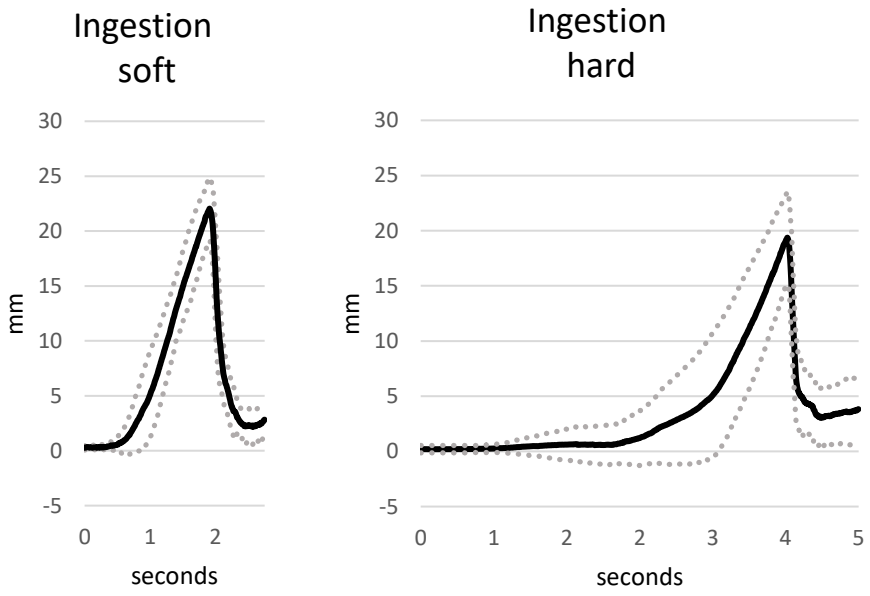

Fig. 21. The mean value graphs depict the ingestion of *C. mouhotii*. The y-axis shows the distance between the tracking points set on the upper- and the lower jaw. The dotted lines show the standard deviation. Zero marks the point at which the jaws are closed and relaxed. The ingestion is separated into two phases, mouth opening and mouth closing.

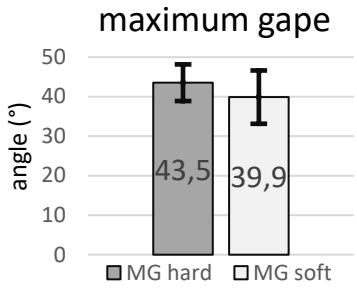

Fig. 22. Displayed are the maximum gape angles during ingestion of *C. mouhotii*, feeding terrestrial on hard and soft food.

Tab. 1. Depicted is the data of the **ingestion** of *C. mouhotii*. The phase is subdivided into an opening and a closing phase. Data for opening, closing and the whole cycle are shown for both hard (snails) and soft (peach) food. Beneath each row the standard deviation is displayed. Duration (green) in seconds; The max velocity (red) is composed of the 10 highest speeds of each individual film, again averaged for all videos.

Phase	Duration (s)	mean velocity (mm/s)	max velocity (10) (mm/s)
Mean open soft	0,969	18,447	64,290
SD open soft	0,204	12,449	16,446
Mean open hard	1,333	16,539	78,199
SD open hard	0,743	5,133	17,695
Mean close soft	0,438	49,801	193,713
SD close soft	0,207	19,218	48,046
Mean close hard	0,176	105,864	272,375
SD close hard	0,090	43,214	83,197
Mean cycle soft	1,376		
SD cycle soft	0,338		
Mean cycle hard	1,592		
SD cycle hard	0,704		

The TP started with a SO of the jaws, which lessened in speed after about half a second, while simultaneously protracting the tongue to the tip of the upper jaw and beyond. This was followed by the FO. Almost the same duration occur with both food sources. Slight differences in inclination and amplitude are detectable, but in contrast to the ingestion and the MP, this feeding phase is the most stereotype and uniform (Figs. 23; 25; 26). The whole cycle was 1,287 s for soft food and 1,243 s for hard food. The maximum speed was reached again during closing with 215 mm/s for hard food. The FO achieved a six times higher speed compared to the SO. The highest velocities in the TP were also found in its closing phase, resulting in a mean velocity of 69,6 mm/s (Tab. 2). Sometimes, at the first TP the head was stretched out again during FO (Fig. 25).

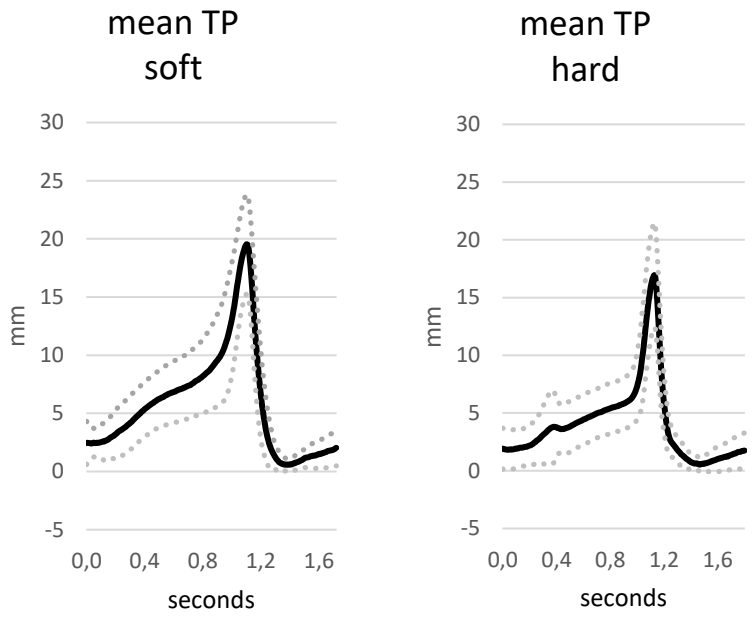

Fig. 23. Transport phases of soft and hard food resemble each other in appearance in *C. mouhotii*. The dotted lines indicate the standard deviation. The TP shows a slow opening phase followed by a fast opening and a closing phase.

Tab. 2. The data of *C.mouhotii's* **transport phase** is shown. The phase is subdivided into slow opening (SO), fast opening (FO) and closing. Data for opening, closing and the whole cycle are shown for both hard (snails) and soft (peach) food. Beneath each row the standard deviation is displayed. Duration (green) in seconds; The max velocity (red) is composed of the 10 highest speeds of each individual film, again averaged for all videos.

Phase	Duration (s)	mean velocity (mm/s)	max velocity (10) (mm/s)
Mean SO soft	0,806	9,377	53,341
SD SO soft	0,224	4,504	23,006
Mean SO hard	0,709	9,178	45,567
SD SO hard	0,228	8,822	25,236
Mean FO soft	0,231	53,239	113,195
SD FO soft	0,082	16,772	35,721
Mean FO hard	0,194	61,290	120,513
SD FO hard	0,134	27,857	50,559
Mean close soft	0,271	70,991	204,303
SD close soft	0,052	22,290	66,103
Mean close hard	0,284	68,273	215,420
SD close hard	0,208	36,852	85,648
Mean cycle soft	1,287		
SD cycle soft	0,243		
Mean cycle hard	1,243		
SD cycle hard	0,245		

Manipulation occurred when the food item was not correctly positioned in the mouth or when snail shells were not broken up enough. The MP, which separated only into an opening and closing phase, were shorter when feeding on hard food. The averaged MP graphs reflected the same scheme. Amplitude as well as appearance of the two MP were different (Fig. 24). Interestingly, mean velocities were higher for soft food. The maximum velocities showed the same trend (Tab. 3).

Especially in hard food, namely the snails, MP were observed more often. Differences in appearance of the MP to the TP are visualized in figure 26.

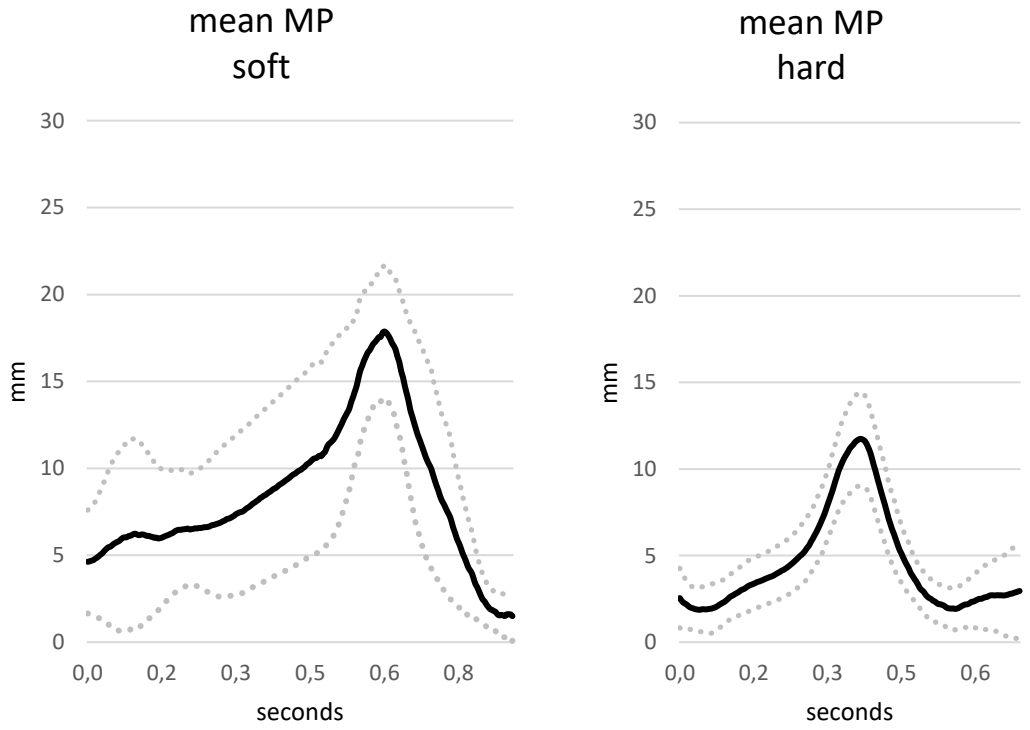

Fig. 24. Means of the manipulation phases (MP) during feeding in *C. mouhotii* are depicted. Dotted lines indicate the standard deviation. The y-axis marks the distance between the lower and upper jaw. Hard food MP shows a lower amplitude and duration than the soft food MP.

Tab. 3. Data of the **manipulation phase** is displayed in the feeding cycle of *C. mouhotii*. Data for opening, closing and the whole cycle are shown for both hard (snails) and soft (peach) food. Beneath each row the standard deviation is displayed. Duration (green) in seconds; The max velocity (red) is composed of the 10 highest speeds of each individual film, again averaged for all videos

Phase	Duration (s)	mean velocity (mm/s)	max velocity (10) (mm/s)
Mean open soft	0,621	30,079	97,667
SD open soft	0,224	6,563	22,235
Mean open hard	0,406	27,290	83,588
SD open hard	0,158	9,295	21,939
Mean close soft	0,288	76,352	185,824
SD close soft	0,158	37,125	74,455
Mean close hard	0,237	50,355	111,373
SD close hard	0,103	24,556	34,795
Mean cycle soft	1,032		
SD cycle soft	0,147		
Mean cycle hard	0,807		
SD cycle hard	0,332		

The movements of the tongue were only evaluated during the TP. In the individual film graphs, it is clearly visible that with every TP a protraction, a plateau phase and a retraction of the tongue appeared. This typical movement of the tongue differentiates the TP clearly from the MP, where the tongue movement lacked a plateau phase (Fig. 26). So, the most prominent and best measurable feature of that tongue movement was the plateau phase. *C. mouhotii* protracted its tongue during the SO and pressed it on the roof of the mouth cavity, where it locked its prey into position, and slid the tongue even further anterior. Until maximum gape was reached, the tip of the tongue was still at the tip (or further anterior) of the upper jaw. Simultaneously to the start of the closing phase the tongue was quickly retracted. The prey lost connection to the roof of the mouth and stuck to the tongue. With this reoccurring cycle the turtle was able to transport the prey further backwards in the mouth cavity. After several TP cycles it reached a position where it could be swallowed. The plateau phase of the tongue, where it rested at the roof of the mouth cavity, had roughly the same duration with soft (0,441 s) and hard food (0,423 s) (Tab. 4).

Tab. 4. Data of the the **tongue movement** of *C. mouhotii* during the transport phase of the feeding cycle is shown. Data for protraction, the plateau phase and the retraction are shown for both hard (snails) and soft (peach) food. Beneath each row the standard deviation is displayed. Duration (green) in seconds; The max velocity (red) is composed of the 10 highest speeds of each individual film, again averaged for all videos.

Phase	Duration (s)	mean velocity (mm/s)	max velocity (10) (mm/s)
Mean protr. soft	0,274	20,701	54,691
SD protr. Soft	0,123	9,081	31,825
Mean protr. hard	0,255	25,432	63,636
SD protr. hard	0,127	24,035	34,061
Mean plateau soft	0,441		
SD plateau soft	0,172		
Mean plateau hard	0,423		
SD plateau hard	0,172		
Mean retr. soft	0,135	52,230	104,492
SD retr. soft	0,047	19,835	29,526
Mean retr. hard	0,117	69,646	117,478
SD retr. hard	0,037	29,762	40,518

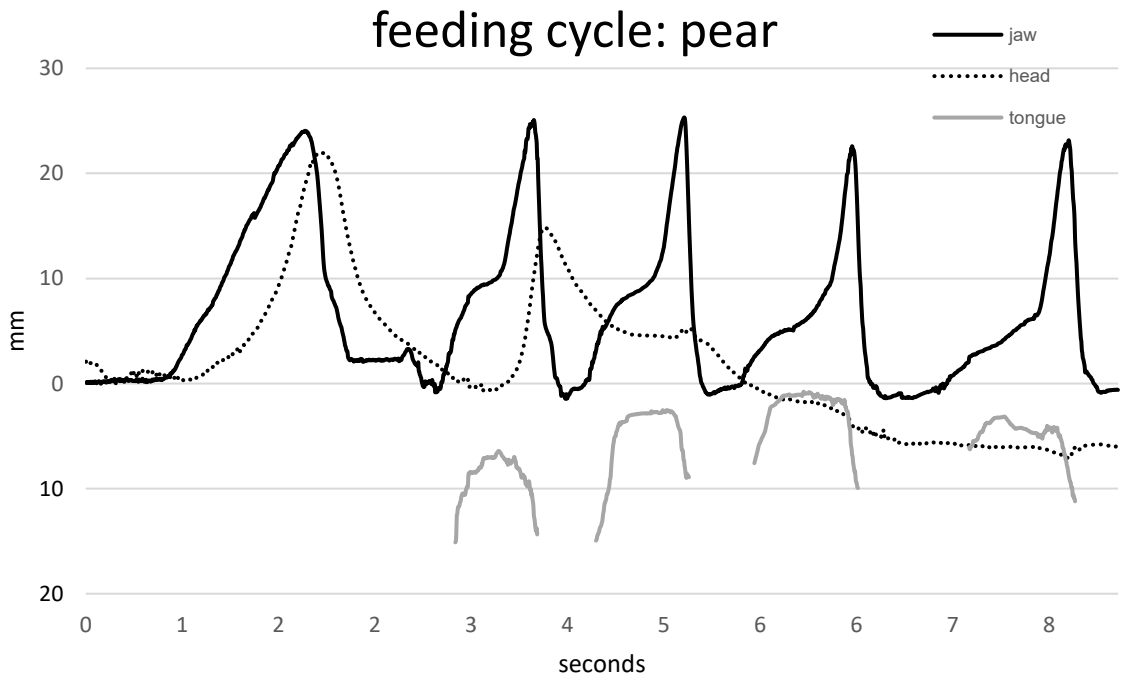

Fig. 25. Kinematic profile of one complete feeding cycle of *C. mouhotii*, feeding on a small slice of pear. The zero point is chosen at the start of the cycle when the jaws (black line) are still closed. The y-axis depicts the amplitude of two points to each other, e.g. lower and upper jaw. The first peak at 2 seconds shows the ingestion, closely followed by the dotted line peak (head) which has its maximum protraction shortly after the maximum gape. The turtle reaches over the food with the head and grasps it with its beak. At this point the tongue (grey line) is not visible and far back in the mouth. The tongue protracts and retracts with a plateau phase in between at the next four gape peaks. These plateau phases and pressing the tongue against the palate and vomer are typical for the TP. The TP itself is divided into three stages seen at the last four peaks. These phases cycle until the prey gets to a position in the mouth were it can be swallowed.

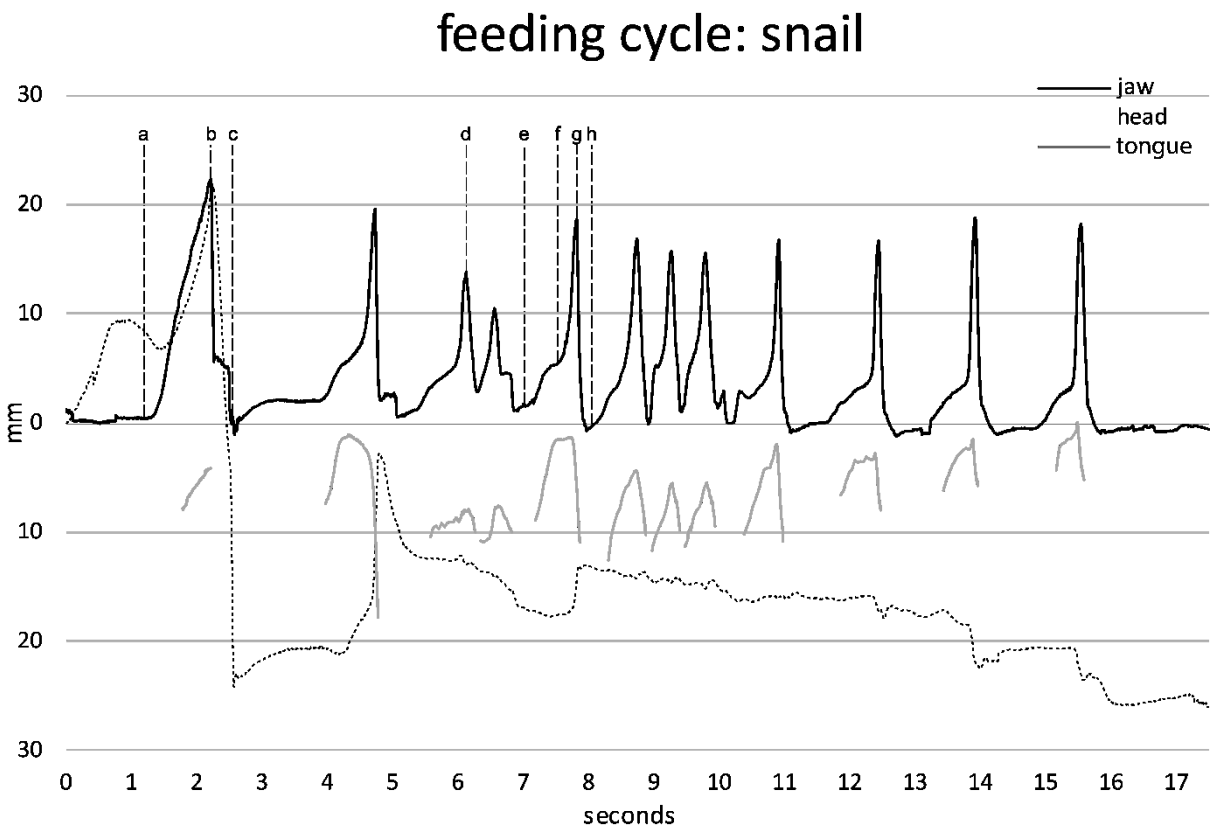

Fig. 26. The depicted graph of the mouth opening, head movement, and tongue movement shows a typical feeding cycle of *C. mouhotii* with hard food, namely a snail. The first peak (at 2 sec.) on the black line (jaw movement) illustrates the ingestion, which is a steady opening followed by a fast grasping of the snail, which then was crushed with a power stroke, depicted by a small bump in the closing phase. The tongue (grey line) was only slightly visible during ingestion and the movement corresponds to the lowering of the jaw. The head movement (black dotted line) indicates a fast retraction because of a small shock when the turtle crushed the snails shell. The following peak shows a transport phase (at 5 sec.) with its corresponding tongue movement. A fast protraction and retraction with a plateau phase in between are typical. At 5,5-7 seconds, two manipulation phases are visible, which do not show the typical tongue movement of TP, the protraction and retraction are weaker in comparison. Manipulation and transport then alternate and the whole feeding cycle ends in four transport phases, seen in the last four peaks of the jaw movement. Letters a-h correspond to the pictures of the feeding cycle in Figure 27.

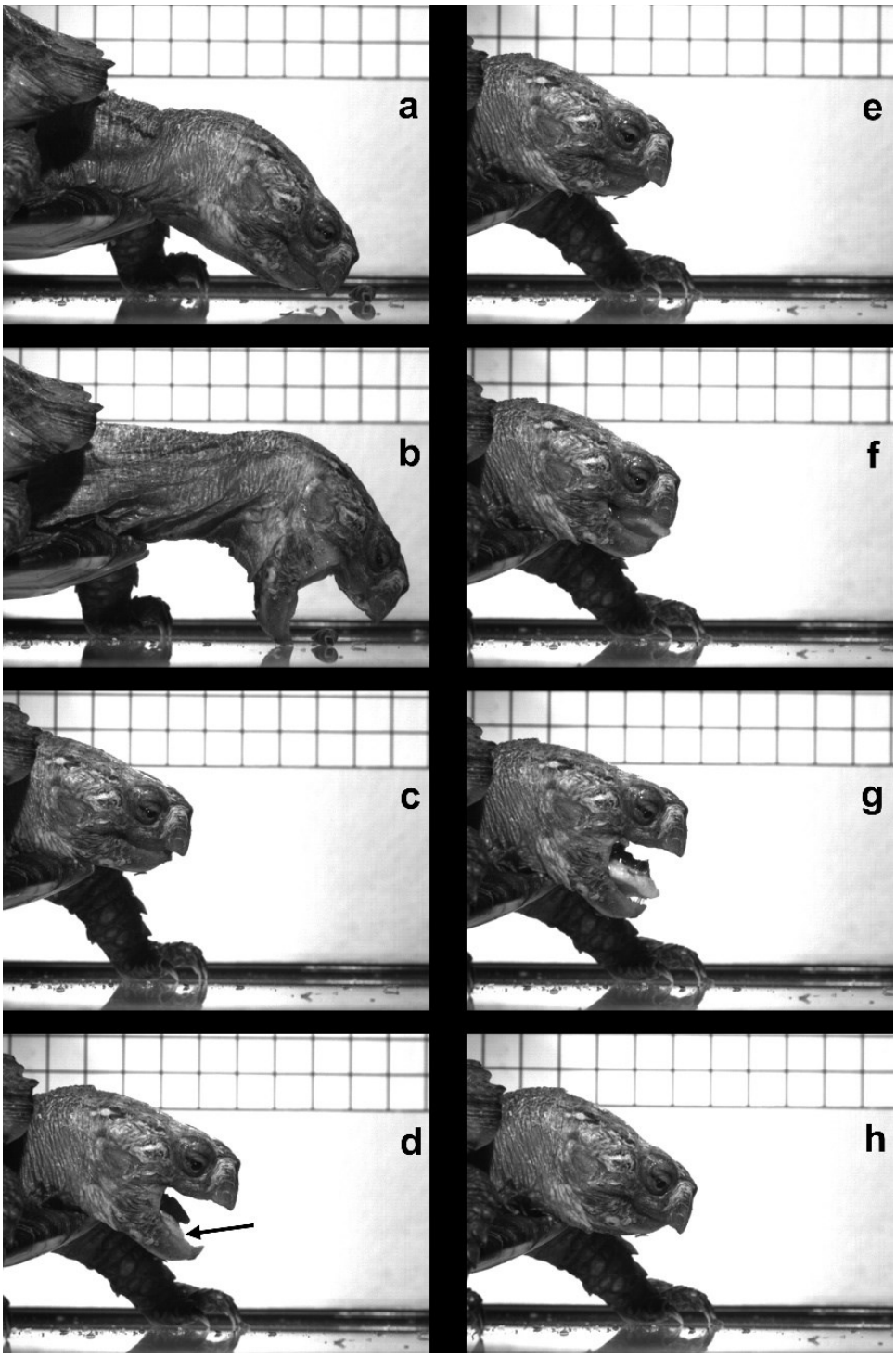

Fig. 27. Feeding cycle of *C. mouhotii* with a snail as prey. Pictures are according to the feeding cycle displayed in Fig. 26. (a) before the start of the ingestion the turtle approaches the prey; (b) maximum gape is reached, the neck is bent and the head points towards the ground and the prey; (c) closing of the mouth and retraction of the neck; (d) MP, the jaws are opened and the tongue directs the snail to the rhamphotheca where it can be broken up further; note the lowered position of the tongue (arrow); (e) closing of the mouth; (f) slow open phase in the TP and protraction of the tongue to the tip of the upper jaw; (g) fast opening with simultaneous retraction of the tongue and detachment of the prey from the palate; (h) complete closing of the mouth after the TP.

4.2.1. Aquatic feeding

For several weeks all individuals were tested for their ability to feed under water. With a stone as a safety structure in the aquarium and a water temperature of about 27°C the turtles appeared to relax in the aquatic setup. In lower temperatures or when they lost touch with the ground, they pedalled constantly and could neither relax nor concentrate on the prey presented to them under the water surface. Different food sources were used: snails, fruits, mealworms and fish, but it seemed that *C. mouhotii* was again the most eager for snails. Only two individuals were willing to observe the food with opened eyes under the water surface, which turned out to be the only possible way to aim correctly. Spotting the food from above the water surface did lead to a miss aiming due to the refraction of air to water. Two individuals went for the prey several times, but less frequent compared to terrestrial feeding. Sometimes they even managed to grasp the prey by the jaws, followed by insufficient TP and MP. They did not manage to complete a full feeding cycle under water. The prey was then removed from the mouth cavity by its fore claws. Over some weeks of testing, only two films with an incomplete feeding cycle were produced. These two films were used for measuring the ingestion. Unfortunately, these two inconsistent films were not enough for comparative data analyses. Nevertheless, the small data set resulted in durations and velocities in the same range of terrestrial feeding and ingestion. Neither the mouth opening, nor the closing are faster in water compared to terrestrial ingestion. These two films and the observation of my other film material led to the finding that they are not able to use suction feed. The mouth cavity naturally completely fills with water, but there is no rapid hyoid depression and the prey right in front of the mouth is not moving any further to the mouth. Swallowing was never observed under water. When the animals stretched their heads above the water surface to get rid of water they swallowed parts of the prey. Overall, they did not seem to have either the coordination necessary for underwater suction feeding or the morphological or behavioural requisites to do so. *C. mouhotii* was eager for the prey but could not manage to fulfil a full underwater feeding cycle by ram feeding, by suction feeding or by compensatory suction feeding.

5. Discussion

5.1. Skull morphology within the genus *Cuora*

Cuora mouhotii's morphology does resemble one of a typical *Cuora* species, with a rather elongated, dorsally flattened head, a connection between quadratojugal and postorbital, and caudally elongated supraoccipital (for comparison see Gaffney, 1979; Natchev et al., 2009). Foth et al. (2017) showed, that only slight changes in skull shape in turtles are necessary to adapt to different environments. At first glance *Cuora* skulls look similar, only slight differences in between the genus *Cuora* head morphology are detectable. These small differences are appearing due to the species habitat and the feeding mode (Claude et al., 2004; Foth et al., 2017). Three *Cuora* species were already studied regarding there feeding mechanisms (Natchev, 2004; Natchev et al., 2007, 2009): *C. galbinifrons*, *C. flavomarginata* (Ota et al., 2009) and *C. amboinensis,* which inhabit environments from wetlands (*C. amboinensis*) (Schoppe & Das, 2011) to terrestrial evergreen forests (*C. galbinifrons*) (McCormack et al. 2016). *C. amboinensis* in contrast to the other investigated species has a dorsally flatter skull. As an aquatic feeder it needs to minimize water turbulences during suction feeding, thus a flattened skull can partly prevent this issue (Bramble, 1973). Following Claude et al. (2004), particularly in *Cuora* environmental dependent skull shapes are present from aquatic to terrestrial. Within the genus *Cuora*, terrestrial skulls possess a dorsal curvature between the posterior supraoccipital and the anterior parietal, like in *C. flavomarginata* (Natchev, 2004) and *C. mouhotii* (Gaffney, 1979).

In *C. amboinensis* the palatine is thick and shows a flat form. In *C. flavomarginata* as well as in *C. galbinifrons* the palatine is concave and thin (Natchev et al., 2009). The flattened palatine could be an indication for an aquatic feeder, where the prey does not need to be pressed against the palatine during the TP and the flat surface does not cause turbulences during suction feeding (Bramble & Wake, 1985). In contrast, typical terrestrial species possess a vaulted palate (Bramble & Wake, 1985), like *C. galbinifrons, C. mouhotii* and *C. flavomarginata*. At least *C. mouhotii* feeds regularly on snails, indicating a need for a stronger palate to prevent harm in the oral cavity when crushing shells.

An indication for a strong adductor mandibulae complex is a crista reaching ventrally of the basisphenoid, where the amipptp and amipptv have their origin. *Heosemis grandis*, another geoemydid turtle feeding on land and in water, shows a flat bone without a distinct crista (Lintner et al., 2012).

5.2. The adductor mandibulae complex

The muscle "system" as proposed by Werneburg (2011) was found to fit for *Cuora mouhotii* quite well. The adductor mandibulae externus complex is strong and massive in this species. In general, the biggest part of the bite force must be produced by the two muscles amepp and ameps. Observing the specimen during feeding clearly showed a compression when closing the jaws, especially when crushing big snail shells during MP. When doing so, an increase in volume on the posterior dorsal part of the head was visible. These observations are confirmed by electromyography activity patterns of tetrapods, which show an activity of the external adductor complex during closing of the jaws (Bramble & Wake, 1985). Even though the supraoccipital is enlarged posteriorly, the adductor mandibulae externus does span even further posterior. This posterior enlargement and the great muscle volume and mass do indicate a diet were high bite forces are obligatory. The insertion of the amepp and ameps on the lower jaw is rather small in relation to their origin, but a lack of attachment sites is compensated for by the large surface area on the coronar aponeurosis in the sagittal axis. The forces are spread at the insertion as well as at the origin over a large area, so the turtle can create higher forces while not harming itself when these muscles are in full tension. Pulling forces on the lower jaw are directed from a horizontal direction dorsally into a more dorsoventral direction. This is accomplished by the coronar aponeurosis, which has a myovector changing function. The anterior-posterior force vector at the dorsoposterior part of the skull created by the amepp and ameps is transferred into an upward force, which is likely a preferable force vector direction for the jaw-closing mechanism (Fig. 12). The biggest part of these muscles lies posterior to the temporal fossa, therefore it is necessary that the horizontal force vector becomes vertical, in order to lift the mandible (Schuhmacher, 1973; Bramble, 1974; Lemell et al., 2000). Neither a cartilaginous element, namely the cartilago transiliens, as described for *Chelone* and *Caretta* (Schuhmacher, 1953), *Testudo hermanni boettgeri* (Wochesländer et al., 1999) and different other chelonian species (Schuhmacher, 1956, 1973; Gaffney, 1975), nor an Os transiliens, as reported for *Gopherus polyphemus* (Ray, 1959), can be found in *C. mouhotii*. Here, the tissue does not change its texture in any form to the surrounding, and the tomographical appearance of this tendon does not resemble that of other cartilages. Thus, the microCT scans show no indication of a cartilaginous tissue or ossification within the coronar aponeurosis. The same situation is found in *C. galbinifrons* (Natchev et al., 2010). On the contrary, *C. flavomarginata* (Natchev, 2004) and *C. amboinensis* (Natchev et al., 2009) both possess a cartilago transiliens. As with *C. mouhotii*, the semi-aquatic *C. amboinensis* possesses a comparatively big ame to catch and hold onto elusive prey in water (Natchev et al., 2009). In contrast to that, the ame

complex is smaller in *C. flavomarginata* and *C. galbinifrons*. Their diet is mainly omnivorous and mostly has a soft consistency (Ota et al., 2009, McCormack et al., 2016), hence biting does not need the same amount of force like crushing snails in *C. mouhotii*. This indicates a trend in muscle volume or bite force regarding their diet, but - at least for *Cuora* - not regarding the environment.

The amepm was not distinguishable in the microCT data from other ame muscles, only the dissection showed fibres belonging to the amepm. Natchev (2004) did find a clear separation of the amepm and the ameps in *C. flavomarginata*, whereas Poglayen-Neuwall (1953) described this portion as weak in *Cuora* compared to other turtles.

The plesiomorphic condition of the ame and ami is said to be that the adductor mandibulae portions are separated by the N V_3 (Holliday & Witmer, 2007), which is consistent with the findings in *C. mouhotii*. All reports so far in *C. amboinensis* and *C. flavomarginata* report the V_2 lateral of the amipps and amippss (Poglayen-Neuwall, 1953; Natchev, 2004). *C. mouhotii* displayed a split of the amipps portions by the V_2. This means that the V_2 switched its position between two ami muscles and not the internus complex medially and the externus complex laterally, as was reported for different turtles (Poglayen-Neuwall, 1953; Iordansky, 1996). Though this condition can vary between the two sides of one individual.

The amipi is present and connected to the intapo, which typically is in contact to the amippt dorsally (Poglayen-Neuwall, 1953). So far, this muscle was not described for other *Cuora* species (Poglayen-Neuwall 1953; Natchev, 2004; Natchev et al., 2009). It is only a slim muscle portion, which is separated from the pseudotemporalis muscle by the small but distinct intapo. Even though the amippt is parted into two portions beneath the pterygoideus (Iordansky, 2010; Werneburg, 2011), the separation of the ventral and the posterior portion was only possible at its origin. Therefore, 3D visualisations (Fig. 9) show one muscle including both portions. In *C. amboinensis* a separation of the amipps and the amippt was not found (Natchev et al., 2009). MicroCT scanning methods could help to get a clearer picture of these muscle portions. Differences of innervation patterns regarding amp and ami led to the exclusion of amp from the internus complex, for a comparison see Werneburg (2011). In some turtle species, Schumacher (1953) assigned fibres of the amipps to the amp, which led to the inclusion of the amp to the ami complex. In *C. mouhotii*, the amipps have a dorsoventral orientation going up to the parietal, whereas the amp has its origin at the quadratum and reaches anterioventrally. They are not innervated by the same nerve and thus it is reasonable to exclude the amp from the internus adductor muscles (Rieppel, 1990). In contrast to that, a closer revision of the amp in *C. mouhotii* shows a conjunction of at least some fibres to the ami muscles, namely amipptd, amipptv and

amipptp. This would recommend an inclusion of these muscles to the internus complex for *C. mouhotii*, like Iordansky (2010) stated for turtles. At least for *C. mouhotii* I would reconsider naming this particular muscle ami pars posterior. Nevertheless, muscles are more or less in a "fluid" state and change their appearance regularly during growth and ontogeny as proposed by Werneburg (2011). Thus, it is likely that in another individual or even at a different age these muscles are not connected. As in *C. mouhotii*, only one portion of the amp was found in *C. flavomarginata* (Natchev et al., 2009).

In general, all adductor muscles are involved in the closing mechanism of the jaws (Bramble & Wake, 1985). For a complete closing it is crucial that all these muscle portions work together properly, each to a different degree. Most probably the ame creates the highest forces on the lower jaw, judged by its sheer size (Schuhmacher, 1973). The amippt attaches to the lower jaw posterior to the ame. Contracting this internus muscle portions results in a protraction of the mandible. In combination with the retraction of the mandible by the ame, high forces adduct the lower jaw (Iordansky, 1996). These two directions of pulling forces are protecting the jaw of too much stress on the jaw joint itself (Schuhmacher, 1973; Lemell et al., 2000). The amp does create an upward force on the most posterior part, anterior of the jaw joint. Nevertheless, amipps and amippss have a multidirectional arrangement function with the lower jaw, at which they play together with the amipi (Werneburg, 2011). The jaw joint itself is only moveable in a posterior-anterior direction and due to its anatomy can only perform small marginal sheerings, or lateral movements.

It seems that in turtles the m. intermandibularis can vary a bit in its connection or unitedness with other muscles like m. constrictor colli and the m. intramandibularis. Fusions are possible (Rieppel, 1990; Werneburg, 2011), but were not observed in this species.

M. depressor mandibulae and m. dilitator tubae are the antagonists to the adductor mandibulae. They attach to the lower jaw, posterior to the jaw joint. By creating an upward force on the most posterior part of the lower jaw, the anterior part is lowered over the jaw joint. In tetrapods, foremost at the stage of FO, cervico-cranial muscles elevate the skull over the cervic-cranial joint to achieve a big gape angle in the TP (Bramble & Wake, 1985). A slight elevation of the skull during FO can be seen but was not observed during ingestion in *C. mouhotii.*

5.3. The hyoid complex

Hyoid movement was not measured in this study, nevertheless the hyoid and its muscles are clearly involved in the feeding process of *C. mouhotii*. The hyoid musculature plays an important role for protraction of the tongue during MP and TP. Part of the forward movement

of the hyoid complex and therefore the tongue is done by the tension of the m. intermandibularis, which stabilizes the floor of the mouth against forces of other hyoid muscles. A crucial part in this forward movement plays the m. genioglossus (gg) in combination with the m. geniohyoideus (gh). In aquatic turtles like *C. amboinensis* it has been shown (Natchev et al., 2009), that the gh spans up to the tip of the mandible and causes a forward pulling force on the hyoid itself (Lemell et al., 2002). This connection to the mandible could not be detected in *C. mouhotii*, which either indicates a different function of the gh muscle in this species, or an interaction between two muscles. Here, an interplay between the gg and the gh is suggested, which then could fulfil the same functional role as the gh could on his own. Lintner et al. (2012) revealed this mechanism for *Heosemys grandis* (Geoemydidae). A complete functional redirection of the gh would be unlikely, the parsimonious approach of an interaction seems more likely. E.g. in *Manouria emys* (Testdudinidae) (Heiss et al., 2011) the gh is attached to the mandible.

The hyoid, as well as the tongue play together especially during TP and MP. In aquatic feeders, backward hyoid movement and expanding the hyoid laterally is crucial for generating suction forces. When feeding on land the hyoid is still involved but to a lesser extent. In water, m. branchiomandibularis visceralis as well as m. branchiohyoideus are active when the mouth opens and stretch the cb-I laterally. M. coracohyoideus pulls the hyoid posterior (Aerts, 2001). This mechanism is probably slightly adapted for terrestrial feeding, but the same muscles are still found at their respective sites, suggesting a likewise activity pattern. During ingestion on land, the tongue and the hyoid apparatus play an insignificant role. Like in all other Geoemydidae and Emydidae observed so far, the tongue is not involved (for review see: Natchev et al. 2015).

In geoemydids, the ossification process of the hyoid progresses during aging of these turtles. Juveniles mostly possess a cartilaginous hyoid bone, where only one part of the hyoid complex, the cb-I, is ossified (Richter et al., 2007). The skull of the investigated specimen of *C. mouhotii* shows a similar pattern. The probably still subadult individual has an ossified cb-I but no other ossified parts. Richter et al. (2007) displayed a *C. mouhotii* hyoid apparatus with ossified parts in the corpus hyoidei and the cb-II. In *Cuora galbinifrons* it is shown that the hyoid is ossifying almost completely during adulthood (Richter et al., 2007), even though it is a highly terrestrial geoemydid, which still can feed in water (Natchev et al., 2009). This supports an ontogenetic increase in ossification of the hyoid apparatus in the Genus *Cuora* and especially in *Cuora mouhotii*. Although, this statement is not automatically applicable for all other *Cuora* species. Generally, the amount of ossification or the robustness of the hyoid indicates a terrestrial or

aquatic lifestyle. Hyoids of terrestrial species tend to be cartilaginous due to flexibility reasons regarding the tongue movement. An ossified hyoid may counter a flexible, fleshy tongue which is needed for terrestrial food transport and packaging, whereas aquatic forms need strong and stable hyoids for suction feeding or compensatory suction feeding. This general morphological pattern is suggested for a hypothetical tetrapod (Bramble & Wake, 1985; Natchev et al., 2009), and can be found in turtles as well (Lemell et al., 2000; Lemell et al., 2019). The ossification of the hyoid in *C. mouhotii* and in the closely related *C. galbinifrons* stays in contrast to the hypothesis mentioned above. In both, plesiomorphic characters of this trait could be the reason for the ossification. These turtles are secondarily terrestrial, so their common ancestor is said to be aquatic (Claude et al., 2003).

Although it is clear that hyoid- and tongue movement do correspond, the hyoid movement in *C. mouhotii* was not measured due to a difficulty in localization of the hyoid in the video sequences. Often when dealing with snails the turtles did retract their head far back (Fig. 26) until the plastron almost touched their lower jaw, making it impossible to track hyoid movements. Bramble and Wake (1985) suggest that the hyoid is attached to median elements such as the pharynx to provide more structure and rigidness in aquatic species. In *C. mouhotii* elements of the hyoid complex like the cb-II and the trachea are connected via m. geniohyoideus and m. geniohyoideus pars lateralis. This characteristic resembles a more aquatic hyoid structure, which stands a bit in contrast to its terrestrial lifestyle. The, for a terrestrial turtle, relatively large hyoid of *C. mouhotii*, which is quite similar to that of other *Cuora* species like *C. amboinensis*, *C. galbinifrons* (Natchev et al. 2009; Heiss et al., 2010) and *C. flavomarginata* seems like a plesiomorphic trait (Richter et al., 2007). Taking a look at aquatic chelonians like *Chelus fimbriatus* (Lemell et al., 2010) or *Chelodina longicollis* (Aerts, 2001), the hyoid morphology of the genus *Cuora* presents itself as a more terrestrial or semiaquatic hyoid. This hardens the idea that hyoid morphology is not the essential trait within the genus *Cuora* that discriminates terrestrial and aquatic species. Since it is possible for the studied *C. mouhotii* to feed terrestrial with the more or less same hyoid morphology as e.g. *C. amboinensis*, the hyoid morphology and the ossification may not matter as much as tongue morphology, tongue- and hyoid supporting muscles and inherited food intake mechanisms. Only small differences, like fenestrations, in the hypoglossum of *C. flavomarginata* appear, to which information about its function is missing in the literature. Due to a lack of key information about the proportion of the hyoid apparatus relative to the skull it is not completely clear if maybe the size of the hyoid plays a key role in suction feeding or compensatory suction feeding in *Cuora*.

5.4. Other morphological features

The ridges on the vomer as well as the concave palate on the dorsal part of the mouth cavity are probably used when transporting food (Schwenk, 2000). During the TP the tongue presses the food against the roof of the mouth. The concave palate may has its function in trapping food, while sliding the tongue further anterior under the prey (Bramble & Wake, 1985). Due to adhesive forces between the tongue and the food the prey is then released from the palate.
For feeding on snails and arthropods the rhamphotheca is robust and thick. The keratinous beak stretches a bit posterior, anterior to the choanae, alike seen in *C. amboinensis* (Heiss et al., 2008), and helps the turtles crush snails in their mouth during MP. Further enhancing the ability to crush snails is the sharp, pointed beak. Even though the rhamphotheca of *C. flavomarginata* (Poglayen-Neuwall, 1953) and *C. galbinifrons* (Natchev et al., 2009) look similar, the beak itself is not formed as sharp as in *C. mouhotii*.

Cuora mouhotii is able to protract its highly flexible tongue out of the oral cavity. Though the tongue is never used in the initial food uptake, it is essential for manipulation of food in a terrestrial environment. High thin papillae on its surface increase the surface area, and therefore increase adhesive forces combined with mucus (Beisser et al., 2004). Papillae are especially long and well developed in terrestrial turtles. When aquatic, papillae are shorter or completely missing (Beisser et al., 1995, 2001; Heiss et al., 2011, Lemell et al., 2010). Bramble & Wake (1985) pointed out that feeding methods as well as morphology are adapted to the respective medium the species feeds in. This principle is applicable for turtles and their tongues as well. In *Cuora* different tongue morphologies appear.

5.5. Kinematics

Head rotations during ingestion as well as head retraction and manipulating snails with their forelimbs turned out to be an issue and interfered with the data analysis. Generally, the individuals were not as eager to feed on fruits as on snails. This supports the observations on the diet of adult *Cuora mouhotii* mainly living carnivorous (Das et al., 2016). As expected, the food grasping mechanisms was the same as for other terrestrial geoemydids, namely jaw prehension. In contrast to emydids which also grasp the food by jaw prehension, the hyolingual complex is retracted (overview in Natchev et al., 2015; Lemell et al., 2019).
As mentioned, *C. mouhotii* is the first reported *Cuora* species to exclusively feed terrestrial. This contradicts Natchev et al. (2009), who propose an inherited tongue based aquatic food transport mechanism for the most terrestrial *Cuora* species. Even though it is not *C.*

flavomarginata, which was suggested by Natchev et al. (2009) to research on next, *C. mouhotii* as a strictly terrestrial species is qualified for investigating these mechanisms as well or even better. *C. flavomarginata* has been reported to enter water from time to time (Ota et al. 2009), a behaviour never seen for *C. mouhotii* except in captivity, mostly shown when they are expected to be in bad health (Das et al., 2016). *C. galbinifrons* is still capable of suction feeding for smaller prey, and only switches to tongue based transport when confronted with larger prey under water (Natchev et al., 2009). I hypothesize that this unique aquatic feeding mechanism is only valid for *C. galbinifrons,* which at least in captivity tends to enter water, and not for all other terrestrial *Cuora* species. *C. galbinifrons* shares a similar high canopy covered habitat with *C. mouhotii* (Xiao et al., 2017a), but dietary preferences differ between both species. *C. mouhotii* tends to a harder structured diet including snails and insects, whereas *C. galbinifrons* skips those as prey (Xiao et al., 2017b). *C. mouhotii* could not create suction forces and tried to use the same feeding mechanisms as in a terrestrial environment, resulting in the loss, or forceful removal of the prey with its claws. It seems like *C. mouhotii* lost its ability to feed aquatic. Even though the ancestor of all *Cuora* was an aquatic species (Claude et al., 2004), the mechanism seems to be successively lost during the evolution of terrestrial *Cuora* species. Advancing the feeding mechanisms for terrestrial feeding seems to go hand in hand with losing or hindering the ability to feed aquatic. The media air and water are very different in its properties resulting in trade-offs for either both or specialisation for one (Bels et al., 2008; Bramble & Wake 1985; Heiss et al., 2018).

5.5.3. Feeding mechanism divided into three stages

Ingestion

Comparing *C. mouhotii's* food intake (1.15 s) with *C. flavomarginata* and *C. amboinensis* (Natchev et al., 2009), the time difference of the whole cycle is striking and was not expected. Both latter mentioned needed only one third of the time to complete the ingestion. *Terrapena carolina* (Emydidae) showed a time to maximum gape of about 0.5 s (Bels et al., 1997; Summers et al., 1998), *Heosemys grandis* (Geoemydidae), judging from the kinematic profiles, of about 0.5 s (Lintner et al., 2010), and *Manouria emys* (Testudinidae) of about 1 – 1.8 s (Natchev et al., 2015). *Testudo hermanni boettgeri* shows compareable mouth opening durations of approximately 1.2 s (Wochesländer et al., 1999). Foremost the mouth opening (time to maximum gape, *sensu* Natchev et al., 2009), but also the closing is prolonged in *C. mouhotii* and thus only comparable with the duration of testudinids, e.g. *Manouria emys* or *Testudo hermanni boettgeri*. One possibility for this behaviour may be that slow velocities and

long times in the feeding cycle allow for more variability. Whereas fast feeding cycles are likely more uniform and stereotypic. Longer cycles allow for the possibility of varying certain parameters depending on prey type. Fast feeding events do not need sensory feedback control, uniformity is key, like in suction feeding. If this principle applies to chelonians as well as to amphibians (Deban et al., 2001) it needs further investigation. *C. mouhotii* is feeding on different food sources and therefore likely to alter its feeding mechanism. If variance in feeding is more likely in prolonged feeding cycles, then it could explain the high standard deviation in the opening phase of the ingestion (Tab. 1). Inter-individually the time as well as the speed of the ingestion changed. For further individual feeding variance see Natchev et al. (2015). Prey dependent alterations are shown for the first time in *Cuora*. This was foremost appearing in the closing of the mouth during ingestion. For aquatic species, prey dependent feeding strategies were already investigated for *Pelusios castaneus* (Lemell & Weisgram, 1997). *C. mouhotii* grabbed snails by the jaws in less than half the time of the peaches. This suggests a sensory feedback, not from the tongue, like in *M. emys* (Natchev et al., 2015), but visually and olfactory, as proposed for other reptiles (Schaerlaeken et al., 2007). Natchev et al. (2015) described tongue-based feeding as the evolutionary speaking "fourth stage" of terrestrial turtle feeding. The extra sensory feedback helps chelonians counter the short loss of sight of the food when approaching, and therefore making the ingestion more "advanced". For testudinid species, mostly feeding herbivorous, this may be true, for other species, especially Emydidae and Geoemydidae with an omnivorous or even carnivorous diet this concept does not seem to fit well. Even in *M. emys* no tongue based food uptake was detected (Natchev et al., 2015). *M. emys* is considered a "transitional turtle" (sensu Natchev, 2015) in respect to its not lingual based feeding mechanism, although it may be that lingual based feeding is not a valid option for omnivorous species. A lingual based feeding mode, be it in Testudinidae or even hypothetical in Geoemydids, namely *C. mouhotii*, would diminish the chances to catch terrestrial elusive prey. Therefore, the most evolutionary advanced modes may be the ones where aquatic feeding was completely lost. This contradicts Natchev (2015), who proposed lingual feeding as the most evolutionary advanced feeding mode. The genus *Cuora* theoretically was placed into the second category, which describes turtles with terrestrial jaw prehension feeding modes which still possess suction feeding mechanisms (Natchev et al., 2015). At least, demonstrated by *C. mouhotii,* not all investigated *Cuora* species still possess an aquatic feeding mode. This would place *C. mouhotii* feeding mechanisms one step ahead, displaying an advanced terrestrial feeding behaviour and a loss of aquatic feeding. Hypothetically, a terrestrial

feeding step ahead of already investigated species like *C. amboinensis, C. flavomarginata* and *C. galbinifrons.*

Transport phase

The general feeding cycle for tetrapods after Bramble & Wake (1985), which indicates an intrinsic feeding behaviour regarding the intraoral transport, was found to fit for *C. mouhotii* as well, although the phases differed from their stereotypical form. In amphibians these divergences from the norm of the general feeding cycle were shown to be the more common state, and therefore the supposed norm turns out to be the exception (Deban et al., 2001). The general appearance of the TP graph looks familiar to the transport model of Schwenk (2000), with some alterations. Only one slow opening instead of SOI and SOII did appear and the closing did sparsely show a power stroke. Differences between soft and hard food are neglectable in the TP. This phase seems uniform and does not vary much between the food regimes, the individuals and the feeding event. Only the amount of TP of each feeding event varies. Snails needed more TP before swallowing, which could be a result of the nature of the presented food, i.e. the snail's mucus, which agglutinated the oral cavity, and the shell.

The investigated species did not show a maximum gape phase (a short plateau phase at the maximum gape position), in contrast to *C. amboinensis* and *C. flavomarginata* (Natchev et al., 2009). *Manuria emys,* a testudinid, shows similar-looking patterns to the latter two mentioned, including a SOI phase and again a maximum gape phase (Natchev et al., 2015). Transport phases were determined by their corresponding tongue movement, which can be found in *C. amboinensis* as well as in *M. emys.* Different tongue movements when processing food led to the additional description of the MP, which differed from the TP.

Manipulating phase

Hardness and sharpness of the snail shells resulted in MP mostly right after the ingestion. The amount, in contrast to peaches as food source, was more than doubled. Before transporting the snails further caudal, they had to be cracked by the rhamphotheca. This thick keratinous structure does reach a bit back in the oral cavity, similar to *C. amboinensis* (Heiss et al., 2008). The jaws cannot move laterally and perform sheering movements (Werneburg, 2011). In that regard a flexible tongue is essential, in a terrestrial environment, to move the prey in a position for the beak to crack it (Schwenk, 2000). This movement does not resemble that of a TP, but is highly variable, and thus, as mentioned, dependent on the food source, and differs each cycle. Nevertheless, the jaw movement during this processing seems quite uniform. With soft food compared to hard food, the gape maximum was higher and the MP cycle duration longer in the

former. Overall, *C. mouhotii* seemed to be more careful when handling snails. Natchev et al. (2009) termed the MP as "prey positioning", but did not link it to the tongue movement but to the extraction of the neck. *C. amboinensis* and *C. flavomarginata* show MP while feeding terrestrial. This alternating feeding mechanism to respond to different food sources appears to be widespread in *Cuora*. Necessity for this is mostly limited to terrestrial environments, while suction feeding or ram feeding is usually followed by transport phases which differ from terrestrial ones (Natchev et al., 2009).

6. Conclusion

This study aimed to provide new insights into the feeding mechanisms in turtles and foremost in the genus *Cuora*. Including already published kinematics and morphological studies on *Cuora,* the picture of the evolution of *Cuora* feeding mechanisms gets clearer with every species investigated. *C. mouhotii* is the first *Cuora* species investigated, which is exclusively able to feed on land. Its feeding behaviour varies regarding the presented food in time as in velocity. That points to a modulation of the different feeding phases, foremost the ingestion and the MP. The ingestion duration resembles the ones of Testudinidae and differs from all other *Cuora* species known so far. This indicates a great possibility for variations in the feeding cycle. The morphological examination of the skull shows only slight differences compared to other *Cuora* skulls. Maybe the modularity of the feeding behaviour affected the adaption to a terrestrial environment even more than morphological adaptions, or slight changes in morphology are enough to provide significant changes in the feeding mechanics and therefore an adaptation to a terrestrial environment.

7. Acknowledgement

First of all, I would like to thank Christian Beisser, my supervisor, for his thoughtful and patient help in every aspect of this thesis. Especially in fields of morphology, kinematics and the tracking software. I am grateful for the help of Patrick Lemell throughout the whole Master-thesis. Constructive discussions in turtle morphology as well as kinematics did improve the content of my thesis greatly. I want to thank both for the support and the introduction to their working group in functional anatomy of vertebrates. Special thanks to

Stephan Handschuh, who carried out the CT Scans and helped me whenever needed. I would like to thank Thomas Schwaha for helping me with Amira and in other different regards. This study would not have been possible without the Tiergarten Schönbrunn and especially Anton Weissenbacher, who provided the specimen for this study. I am grateful to Georg Gassner and the Natural History Museum for lending us the material for the microCT scan.

8. Literature

Aerts, P., Van Damme, J., & Herrel, A. (2001). Intrinsic Mechanics and Control of Fast Cranio-Cervical Movements in Aquatic Feeding Turtles. *American Zoologist, 41*, 1299-1310. doi:https://doi.org/10.1093/icb/41.6.1299

Asian Turtle Trade Working Group (2000). *Cuora mouhotii* (errata version published in 2016). *The IUCN Red List of Threatened Species* 2000: e.T163414A97359633. http://dx.doi.org/10.2305/IUCN.UK.2000.RLTS.T163414A5604435.en.Downloaded on 01 May 2019.

Beisser, C. J., Weisgram, J., & Splechtna, H. (1995). Dorsal lingual epithelium of *Platemys pallidipectoris* (Pleurodira, Chelidae). Journal of Morphology, 226, 267-276. doi: 10.1002/jmor.1052260303

Beisser, C. J., Lemell, P., & Weisgram, J. (2001). Light and transmission electron microscopy of the dorsal lingual epithelium of *Pelusios castaneus* (Pleurodira, Chelidae) with special respect to its feeding mechanics. Tissue Cell, 33(1), 63-71. doi:10.1054/tice.2000.0156

Beisser, C. J., Lemell, P., & Weisgram, J. (2004). The Dorsal Lingual Epithelium of *Rhinoclemmys pulcherrima incisa* (Chelonia, Cryptodira). *The Anatomical Record*., 227A, 227-235. doi:10.1002/ar.a.20008

Bels, V. L., Davenport, J., & Delheusy, V. (1997). Kinematic analysis of the feeding behavior in the box turtle *Terrapene carolina* (L.) (Reptilia: Emydidae). *Journal of Experimental Zoology, 277*(3), 198-212.

Bels, V., Baussart, S., Davenport, J., Shorten, M., O'Riordan, R. M., Renous, S., & Davenport, J. L. (2008). Functional evolution of feeding behavior in turtles. In *Biology of turtles*, 201-226.

Bramble, D. M. (1974). Occurrence and significance of the Os transiliens in Gopher Turtles. *Copeia, 1974*, 102-109.

Bramble, D. M., & Wake, D. B. (1985). Feeding mechanisms of lower tetrapods. In M. Hildebrand, D. M. Bramble, K. F. Liem, & D. B. Wake (Eds.), *Functional vertebrate morphology,* 230-261.

Claude, J., Paradis, E., Tong, H., & Auffray, J.-C. (2003). A geometric morphometric assessment of the effects of environment and cladogenesis on the evolution of the turtle shell. *Biological Journal of the Linnean Society, 79*(3), 485-501. doi:10.1046/j.1095-8312.2003.00198.x

Claude, J., Pritchard, P. C. H., Tong, H., Paradis, E., & Auffray, J.-C. (2004). Ecological Correlates and Evolutionary Divergence in the Skull of Turtles: A Geometric Morphometric Assessment. *Systematic Biology, 53*(6), 933-948. doi:10.1080/10635150490889498

Crawford, N. G., Parham, J. F., Sellas, A. B., Faircloth, B. C., Glenn, T. C., Papenfuss, T. J., Simison, W. B. (2015). A phylogenomic analysis of turtles. *Molecular Phylogenetics and Evolution, 83*(0), 250-257. doi:http://dx.doi.org/10.1016/j.ympev.2014.10.021

Das, I., McCormack, T. E. M., van Dijk, P. P., Hoang, H. V., & Struijk, R. P. J. H. (2016). *Cuora mouhotii* (Gray 1862) – Keeled Box Turtle. *Chelonian Research Monograph, 5*, 099.091-099.012. doi:10.3854/crm.5.099.mouhotii.v1.2016

Deban, S. M., O`Reilly, J. C., & Nishikawa, K. C. (2001). The Evolution of the Motor Control of Feeding in Amphibians. *American Zoologist, 41*, 1280-1298.

Feldman, C. R., & Parham, J. F. (2002). Molecular Phylogenetics of Emydine Turtles: Taxonomic Revision and the Evolution of Shell Kinesis. *Molecular Phylogenetics and Evolution, 22*(3), 388-398. doi:10.1006/mpev.2001.1070

Fischer, I., Wahl, S., Weimer, S., Kuipers, H., Wijk, McCormack, T., Thai,. (2010). Research into the ecology of the Keeled Box Turtle (*Cuora mouhotii*) in Vietnam. University of Applied Sciences Van Hall Larenstein.

Foth, C., Rabi, M., & Joyce, W. G. (2017). Skull shape variation in extant and extinct Testudinata and its relation to habitat and feeding ecology. *Acta Zoologica*, 98, 310-325. doi:10.1111/azo.12181

Fritz, U., Andreas, B., & Lehr, E. (1998). Eine neue Unterart der Dreikiel-Scharnierschildkröte, *Pyxidea mouhotii* (Gray, 1862) (Reptilia: Testudines: Bataguridae). *Zoologische Abhandlungen, Staatliches Museum für Tierkunde Dresden, 50*(3), 33-43.

Fritz, U. & Havaš, P. (2006). Checklist of Chelonians of the World. *CITES Nomenclature Committee.,* German Agency for Nature Conservation.

Fritz, U. & Havaš, P. (2007). *Checklist of Chelonians of the world*.

Fritz, U., Ziegler, T., Herrmann, H., & Lehr, E. (2002). Intergradation between subspecies of *Cuora galbinifrons* Bourret, 1939 and *Pyxidea mouhotii* (Gray, 1862) in southern North Vietnam (Reptilia: Testudines: Geoemydidae). *Faun. Abh. Mus. Tierkd. Dresden, 23*, 59-74.

Gaffney, E. S. (1975). Phylogeny of the Chelydrid Turtles: A Study of Shared Derived Characters in the Skull. *Fieldiana Geology, 33*(9), 157-178.

Gaffney, E. S. (1979). Comparative cranial morphology of recent and fossil turtles. *Bulletin of the American Museum of Natural History., 164*(2), 1-313.

Gray, J. E. (1870). Supplement to the Catalogue of Shield Reptiles in the Collection of the British Museum: Order of the Trustees.

Handschuh, S., Beisser, C. J., Ruthensteiner, B., & Metscher, B. D. (2017). Microscopic dual-energy CT (microDECT): a flexible tool for multichannel ex vivo 3D imaging of biological specimens. *Journal of Microscopy, 267*(1), 3-26. doi:10.1111/jmi.12543

Heiss, E., Aerts, P., & Van Wassenbergh, S. (2018). Aquatic–terrestrial transitions of feeding systems in vertebrates: a mechanical perspective. *Journal of Experimental Biology, 221*(8). doi:10.1242/jeb.154427

Heiss, E., Natchev, N., Beisser, C. J., Lemell, P., & Weisgram, J. (2010). The Fish in the Turtle: On the Functionality of the Oropharynx in the Common Musk Turtle *Sternotherus odoratus* (Chelonia, Kinosternidae) Concerning Feeding and Underwater Respiration. *The Anatomical Record, 293*, 1416-1424.

Heiss, E., Natchev, N., Schwaha, T., Salaberger, D., Lemell, P., Beisser, C. J., & Weisgram, J. (2011). Oropharyngeal Morphology in the Basal Tortoise *Manouria emys emys* With Comments on Form and Function of the Testudinid Tongue. *Journal of Morphology, 272*, 1217-1229.

Heiss, E., Plenk, H. J., & Weisgram, J. (2008). Microanatomy of the Palatal Mucosa of the Semiaquatic Malayan Box Turtle, *Cuora amboinensis*, and Functional Implications. *The Anatomical Record, 291*, 876-885.

Hiiemae, K. M., & Crompton, A. W. (1985). Mastication, food transport, and swallowing. In M. Hildebrand, D. M. Bramble, K. F. Liem, & D. B. Wake (Eds.), *Functional vertebrate morphology*, 262-290.

Holliday, C. M., & Witmer, L. M. (2007). Archosaur adductor chamber evolution: Integration of musculoskeletal and topological criteria in jaw muscle homology. *Journal of Morphology, 268*(6), 457-484. doi:10.1002/jmor.10524

Iordansky, N. N. (1996). Jaw musculature of turtles: Structure, functions, and evolutionary conservatism. *Russian Journal of Herpetology, 3*(1), 49-57.

Iordansky, N. N. (2010). Pterygoideus muscles and other jaw adductors in amphibians and reptiles. *Biology Bulletin, 37*(9), 905-914. doi:10.1134/s1062359010090050

Joyce, W. G. (2015). The origin of turtles: A paleontological perspective. *Journal of Experimental Zoology B., 324*(3), 181-193. doi:10.1002/jez.b.22609

Joyce, W. G., & Gauthier, J. A. (2004). Palaeoecology of Triassic stem turtles sheds new light on turtle origins. *Proceedings of the Royal Society of London B, 271*(1534), 1-5. doi:10.1098/rspb.2003.2523

Joyce, W. G., Rabi, M., Clark, J. M., & Xu, X. (2016). A toothed turtle from the Late Jurassic of China and the global biogeographic history of turtles. *BMC Evolionary Biology, 16*(1), 236. doi:10.1186/s12862-016-0762-5

Kummer, S., Heiss, E., Singer, K., Lemell, P., & Natchev, N. (2017). Feeding behaviour and feeding motorics in subadult European pond turtles (*Emys orbicularis*). *Acta Zoologica Bulgarica, 10*, 77-84.

Le, M., & McCord, W. P. (2008). Phylogenetic relationships and biogeographical history of the genus *Rhinoclemmys* Fitzinger, 1835 and the monophyly of the turtle family Geoemydidae (Testudines: Testudinoidea). *Zoological Journal of the Linnean Society, 153*, 751-767.

Lemell, P., Beisser, C. J., & Weisgram, J. (2000). Morphology and function of the feeding apparatus of *Pelusios castaneus* (Chelonia; Pleurodira). *Journal of Morphology, 244*, 127-135.

Lemell, P., Lemell, C., Snelderwaard, P., Gumpenberger, M., Wochesländer, R., & Weisgram, J. (2002). Feeding patterns of *Chelus fimbriatus* (Pleurodira: Chelidae). *Journal of Experimental Biology, 205*, 1495-1506.

Lemell, P., Natchev, N., Beisser, C. J., & Heiss, E. (2019). Feeding in Turtles: Understanding Terrestrial and Aquatic Feeding in a Diverse but Monophyletic Group. In: Bels, V., & Whishaw, I. Q. (eds) Feeding in Vertebrates. Springer Nature Switzerland, 611-642.

Lemell, P., & Weisgram, J. (1997). Feeding patterns of *Pelusios castaneus* (Chelonia: Pleurodira). *Netherlands Journal of Zoology, 47*(4), 429-441.

Li, C., Wu, X.-C., Rieppel, O., Wang, L.-T., & Zhao, L.-J. (2008). An ancestral turtle from the Late Triassic of southwestern China. *Nature, 456*, 497. doi:10.1038/nature07533

Limaye A. (2012) Drishti: a volume exploration and presentation tool. Proceedings of the Society of Photo-Optical Instrumentation Engineers. 8506, Developments in X-Ray Tomography VIII.

Lintner, M. (2010). Funktionsmorphologische Untersuchungen der Nahrungsaufnahme von *Heosemys grandis*, Gray 1860 (Chelonia, Geoemydidae) mit Berücksichtigung der Ontogenie. (Diploma Thesis)

Lintner, M., Weissenbacher, A., & Heiss, E. (2012). The Oropharyngeal Morphology in the Semiaquatic Giant Asian Pond Turtle, *Heosemys grandis*, and Its Evolutionary Implications. *PLoS ONE, 7*(9), e46344. doi:10.1371/journal.pone.0046344

Lyson, T. R., Joyce, W. G., & Sertich, J. J. W. (2017). A new chelydroid turtle, Lutemys warreni, gen. et sp. nov., from the Upper Cretaceous (Campanian) Kaiparowits Formation of southern utah. *Journal of Vertebrate Paleontology, 37*(6), e1390672. doi:10.1080/02724634.2017.1390672

McCord, W. P., Iverson, J. B., Spinks, P. Q., & Shaffer, H. B. (2000). A New Genus of Geoemydid Turtle from Asia. *Hamadryad, 25*(2), 20-24.

McCormack, T., Shi, H., & Stuart, B. (2016). *Cuora galbinifrons*. The IUCN Red List of Threatened Species 2016: e.T97357437A3078734.

Natchev, N. (2004). Zur Form und Funktion des Kiefer-Zungenbeinapparates bei *Cuora flavomarginata* (Chelonia; Cryptodira). Fakultät für Naturwissenschaften und Mathematik der Universität Wien. (Diploma Thesis).

Natchev, N., Heiss, E., Lemell, P., Stratev, D., & Weisgram, J. (2009). Analysis of prey capture and food transport kinematics in two Asian box turtles, *Cuora amboinensis* and *Cuora flavomarginata* (Chelonia, Geoemydidae), with emphasis on terrestrial feeding patterns. *Zoology, 112*, 113-127.

Natchev, N., Lemell, P., Heiss, E., Beisser, C. J., & Weisgram, J. (2010). Aquatic feeding in a terrestrial turtle: a functional-morphological study of the feeding apparatus in the Indochinese box turtle *Cuora galbinifrons* (Testudines, Geoemydidae). *Zoomorphology, 129*, 111-119.

Natchev, N., Lemell, P., & Weisgram, J. (2007a). Feeding Patterns in *Cuora galbinifrons* (Bourret, 1939). *Journal of Morphology, 268*, 1110.

Natchev, N., Lemell, P., & Weisgram, J. (2007b). Feeding patterns of asian box turtles - a comparative study on *Cuora amboinensis* and *Cuora flavomarginata* (Chelonia, Emydidae). *Journal of Morphology, 268*, 1110.

Natchev, N., Tzankov, N., Werneburg, I., & Heiss, E. (2015). Feeding behaviour in a 'basal' tortoise provides insights on the transitional feeding mode at the dawn of modern land turtle evolution. *PeerJ, 3*, e1172. doi:10.7717/peerj.1172

Ota, H., Yasukawa, Y., Fu, J., & Chen, T. (2009). *Cuora flavomarginata* (Gray 1863)—Yellow-Margined Box Turtle. *Chelonian Research Monograph, 5*, 035.031-035.010. doi:10.3854/crm.5.035.flavomarginata.v1.2009

Pereira, A. G., Sterli, J., Moreira, F. R. R., & Schrago, C. G. (2017). Multilocus phylogeny and statistical biogeography clarify the evolutionary history of major lineages of turtles. *Molecular Phylogenetics and Evolution, 113*, 59-66. doi:10.1016/j.ympev.2017.05.008

Platt, S. G., Platt, K., Myo, K. M., Moe, K., Soe, M. M., Naing, T. Z., Rainwater, T. R. (2013). Noteworthy records of chelonians from the Chindwin river basin and Naga hills of western Myanmar. *Herpetological Conservation and Biology, 8*(2), 335-350.

Poglayen-Neuwall, I. V. O. (1953). Untersuchungen der Kiefermuskulatur und deren Innervation bei Schildkröten. *Acta Zoologica, 34*(3), 241-292. doi:10.1111/j.1463-6395.1953.tb00472.x

Ray, C. E. J. A. A. (1959). A sesamoid bone in the jaw musculature of *Gopherus polyphemus* (Reptilia: Testudiniae).107, 85-91.

Rhodin, A. G. J., Iverson, J. B., Bour, R., Fritz, U., Georges, A., Shaffer, H. B., & Van Dijk, P. P. (2017). Turtles of the world: annotated checklist and atlas of taxonomy, synonymy, distribution, and conservation status. Chelonian Research Monographs 7: 1-292.

Richter, S., Auer, M., & Fritz, U. (2007). Variation of hyoid morphology in geoemydid terrapins. *Amphibia-Reptilia, 28*, 148-153.

Rieppel, O. (1990). The structure and development of the jaw adductor musculature in the turtle *Chelydra serpentina*. *Zoological Journal of the Linnean Society, 98*(1), 27-62. doi:10.1111/j.1096-3642.1990.tb01218.x

Sasaki, T., Yasukawa, Y., Takahashi, K., Miura, S., Shedlock, A. M., & Okada, N. (2006). Extensive Morphological Convergence and Rapid Radiation in the Evolutionary History of the Family Geoemydidae (Old World Pond Turtles) Revealed by SINE Insertion Analysis. *Systematic Biology, 55*(6), 912-927. doi:10.1080/10635150601058014

Schaerlaeken, V., Meyers, J. J., & Herrel, A. (2007). Modulation of prey capture kinematics and the role of lingual sensory feedback in the lizard *Pogona vitticeps*. *Zoology, 110*, 127-138.

Schoch, R. R., & Sues, H.-D. (2015). A Middle Triassic stem-turtle and the evolution of the turtle body plan. *Nature, 523*, 584-587. doi:10.1038/nature14472

Schoppe, S., & Das, I. (2011). *Cuora amboinensis* (Riche in Daudin 1801)–Southeast Asian Box Turtle. *Chelonian Research Monograph, 5*, 053.051-053.013.

Schuhmacher, G. H. (1953). Beiträge zur Kiefermuskulatur der Schildkröten - 1. Mitteilung. *Wissenschaftliche Zeitschrift der Ernst Moritz Arndt-Universität Greifswald, 67*, 464-510.

Schuhmacher, G. H. (1973). The head muscles and hyolaryngeal skeleton of turtles and crocodilians. In C. Gans (Ed.), *Biology of the Reptilia, 4*. London and: Academic Press.

Schuhmacher, G. M. (1956). Morphologische Studie zum Gleitmechanismus des M. adductor mandibularis externus bei Schildkröten. *Anatomischer Anzeiger, 103*, 1-12.

Schwenk, K. (2000). An introduction to tetrapod feeding. In Feeding, 21-61. Academic Press.

Schwenk, K., & Rubega, M. A. (2005). Diversity of Vertebrate Feeding Systems. In J. M. Starck & T. Wang (Eds.), Physiological and ecological adaptations to feeding in *vertebrates* (pp. 1-41). Enfield, New Hampshire: Science Publishers.

Seeley, H. G. (1892). On a new reptile from Welte Vreden (Beaufort West), Eunotosaurus africanus (Seeley(Joyce, 2015)). *Quarterly Journal of the Geological Society*, *48*, 583-585.(Claude et al., 2004)

Shaffer, H. B., McCartney-Melstad, E., Near, T. J., Mount, G. G., & Spinks, P. Q. (2017). Phylogenomic analyses of 539 highly informative loci dates a fully resolved time tree for the major clades of living turtles (Testudines). *Molecular Phylogenetics and Evolution, 115*, 7-15. doi:https://doi.org/10.1016/j.ympev.2017.07.006

Shi, H., Parham,. J. F., Simison, W. B., Wang, J., Gong, S., Fu, B. (2005). A report on the hybridization between two species of threatened Asian box turtles (Testudines: *Cuora*) in the wild on Hainan Island (China) with comments on the origin of 'serrata'-like turtles. *Amphibia-Reptilia*, *26*(3), 377-381.

Shi, H., Parham, J. F., Zhiyong, F., Meiling, H., & Feng, Y. (2008). Evidence for the massive scale of turtle farming in China. *Oryx, 42*(01). doi:10.1017/s0030605308000562

Struijk, R., & Blanck, T. (2016a). A likely new natural hybrid form of "*Cuora serrata*"(*Cuora picturata* x *Cuora mouhotii obsti*) and its finding in the wild in Phu Yen province, Vietnam. *Herpetology Notes, 9*, 73-80.

Struijk, R. P. J. H., McCormack, T. E. M., Nguyen, T. T., Pham, T. V., Stumpel, J. B. G., Wang, J., & Auer, M. (2016b). Intergradation between *Cuora mouhotii mouhotii* (Gray, 1862) and *Cuora mouhotii obsti* Fritz, Andreas & Lehr, 1998 with notes on the species' geographical distribution and phenotypic variation. *Sauria, 38*(1), 31-47.

Stuart, B. L., & Parham, J. F. (2004). Molecular phylogeny of the critically endangered Indochinese box turtle (*Cuora galbinifrons*). *Molecular Phylogenetics and Evolution, 31*, 164-177.

Summers, A. P., Darouian, K. F., Richmond, A. M., & Brainerd, E. L. (1998). Kinematics of aquatic and terrestrial prey capture in *Terrapene carolina*, with implications for the evolution of feeding in cryptodire turtles. *Journal of Experimental Zoology, 281*, 280-287.

Wang, J.-C., Gong, S.-P., Shi, H.-T., Liu, Y.-X., & Zhao, E.-M. (2011). Reproduction and nesting of the endangered keeled box turtle (*Cuora mouhotii*) on Hainan Island, China. *Chelonian Conservation and Biology, 10*(2), 159-164.

Wangyal, J. T., Wangchuk, D., & Das, I. (2012). First Report of Turtles from the Himalayan Kingdom of Bhutan. *Chelonian Conservation and Biology, 11*(2), 268-272. doi:10.2744/ccb-0995.1

Werneburg, I. (2011). The cranial musculature of turtles. *Palaeontologia Electronica, 14*(2), 1-99.

Wochesländer, R. (2001). Feeding mechanism of *Cuora amboinensis* (Chelonia; Cryptodira). *Journal of Morphology, 248*(3), 302.

Wochesländer, R., Gumpenberger, M., & Weisgram, J. (2000). Intraoral food transport in *Testudo hermanni* (Chelonia, Cryptodira) - A radiographic video analysis. *Netherlands Journal of Zoology, 50*(4), 445-454.

Wochesländer, R., Hilgers, H., & Weisgram, J. (1999). Feeding mechanisms of *Testudo hermanni boettgeri* (Chelonia, Cryptodira). *Netherlands Journal of Zoology, 49*(1), 1-13.

Wyneken, J., Godfrey, M. H., & Bels, V. L. (2008). Biology of turtles: CRC Press.Bramble, D. M. (1973). Media dependent feeding in turtles. *American Zoologist, 13*, 1342.

Xiao, F., Wang, J., Long, Z., & Shi, H. (2017b). Diet of Two Endangered Box Turtles (*Cuora* spp.) on Hainan Island, China. *Chelononian Conservation and Biology, 16*(2), 236-238. doi:10.2744/ccb-1246.1

Xiao, F., Wang, J., Shi, H., Long, Z., Lin, L., & Wang, W. (2017a). Ecomorphological correlates of microhabitat selection in two sympatric Asian Box Turtle species (Geoemydidae: *Cuora*). *Canadian Journal of Zoology, 95*(10), 753-758. doi:10.1139/cjz-2016-0218

Zhou, T., Blanck, T., McCord, W. P., & Li, P. P. (2008). Tracking *Cuora mccordi* Ernst, 1988: the first record of its natural habitat; a re-description; with data on captive populations and its vulnerability. *Hamadryad, 32*(1), 57-69.

9. Abbrevation List

ame…adductor mandibulae externus

amepm…pars medialis (17)

amepp…pars profundus (19)

ameps…pars superficialis (21)

ami…adductor mandibulae internus

amipi…pars intramandibularis (25)

amipps…pars pseudotemporalis (23)

amippss…pars pseudotemporalis superficialis (24)

amipptd…pars pterygoideus dorsalis (26)

amipptp…pars pterygoideus posterior (27)

amipptv…pars pterygoideus ventralis (28)

amp…adductor mandibulae posterior (29)

an…angular

ar…articular

bh…m.branchiohyoideus (55)

bm…m.branchiomandibularis (47)

bo…basioccipital

bs…basisphenoid

ca….coronar aponeurosis

cal…carapacoocervico-capitis lateralis pars capitis (81)

cam…carapacoocervico-capitis medialis pars capitis (82)

cb-I…Cornu branchiale-I

cb-II…Cornu branchiale-II

cc…constrictor colli

ch…Corpus hyoidei

co…coracohyoideus (58)

cl…columella

cm…cartilago meckeli

coh…cornu hyale

cr…coronoid

ct…cartilago thyreoidea

dm…depressor mandibulae (45)

dn…dental

dt…dilatator tubae (46)

eb-I…epibranchiale-I

eo…exoccipital

ept…epipterygoid

f…frontal

FO…fast opening

gh…m.geniohyoideus (64)

gg…m.genioglossus (63)

hg…hypoglossum

im…intermandibularis (31)

MG…maximum gape

m.add.man.int….musculus adductor mandibulae internus

m.add.man.ext….musculus adductor mandibulae externus

MP…manipulation phase

mx…maxilla

mxmggl…maxillomandibular ganglion

N I…nervus opticus

N II…nervus olfactorius

N III…nervus occulomotorius

N IV…nervus trochlearis

N V…nervus trigeminus

N V_1…nervus ophthalmicus

N V_2…nervus maxillaris

N V_3…nervus mandibularis

N VI…nervus abducens

N VII…nervus facialis

N VIII…nervus vestibulocochlearis

N IX…nervus glossopharyngeus

N X…nervus vagus

N XI…nervus accesorius

N XII…nervus hypo-glossus

oblinf… obliquus inferior (1)

oblsup… obliquus superior (8)

op…opiotic

pa…parietal

pf…prefrontal

pl…palatine

pm…premaxilla

po…prootic

por….postorbital

pra…prearticular

ppt…processus pterygoideus

pt…pterygoid

qu…quadratum

quc…quadratum cartilage

quj…quadratojugal

recant…rectus anterior (2)

recinf…rectus inferior (3)

recpos…rectus posterior (37)

recsup…rectus superior (4)

retrbulbi…retractor bulbi (38)

sa…surangular

sg…salivary gland

SO…slow opening

so…supraoccipital

squ…squamosal

t…trachea

to…tongue

TP…transport phase

tp…trochlear process

vm…vomer